Nanoscale

REVIEW

View Article Online
View Journal | View Issue

Cite this: *Nanoscale*, 2024, **16**, 1038

Recent progress of heterogeneous catalysts for transfer hydrogenation under the background of carbon neutrality

Guangyu Chen,†[a] Jun Ma,†[a,b] Wanbing Gong, *[a] Jiayi Li,[a] Zheyue Li,[a] Ran Long *[a] and Yujie Xiong *[a,b]

Received 16th October 2023,
Accepted 5th December 2023

DOI: 10.1039/d3nr05207a

rsc.li/nanoscale

Under the background of carbon neutrality, the direct conversion of greenhouse CO_2 to high value added fuels and chemicals is becoming an important and promising technology. Among them, the generation of liquid C1 products (formic acid and methanol) has made great progress; nevertheless, it encounters the problem of how to use it efficiently to solve the overcapacity issue. In this review, we suggest that the catalytic transfer hydrogenation using formic acid and methanol as the hydrogen sources is a critical and potential route for the substitution for the fossil fuel-derived H_2 to generate essential bulk and fine chemicals. We mainly focus on summarizing the recent progress of heterogeneous catalysts in such reactions, including thermal- and photo-catalytic processes. Finally, we also propose some challenges and opportunities for this development.

1. Introduction

The massive increase in the world population inevitably leads to energy shortage and environmental crisis, which is one of the greatest challenges of this century on Earth. The overuse of nonrenewable fossil resources such as coal, oil and natural gas greatly increases CO_2 emission and the accompanying greenhouse effect, and thus it is necessary to develop renewable resources and CO_2 capture and utilization technologies.[1–7] For this, many chemists and materials scientists focus on the development of new renewable resources (wind, light, electricity, *etc.*) and new materials such as nanomaterials. In particular, in the context of carbon neutrality, the highly efficient conversion of CO_2 to formic acid and methanol is regarded as one of the most promising CO_2 direct conversion technologies for industrialization, which is undergoing rapid development.[5,8–14] For example, Yang *et al.* recently synthesized a layered {001}-

[a]*National Synchrotron Radiation Laboratory, School of Nuclear Science and Technology, Hefei National Research Center for Physical Sciences at the Microscale, School of Chemistry and Materials Science, University of Science and Technology of China, Hefei, Anhui 230026, P. R. China. E-mail: yjxiong@ustc.edu.cn, longran@ustc.edu.cn, wbgong2021@ustc.edu.cn*
[b]*Suzhou Institute for Advanced Research, University of Science and Technology of China, Suzhou, Jiangsu 215123, P. R. China*
† These authors contributed equally.

Guangyu Chen

Guangyu Chen received his bachelor's degree in energy chemical engineering from the Hefei University of Technology in 2022. Presently, he is a master's student in Prof. Yujie Xiong's group at the University of Science and Technology of China. His current research interests focus on developing new catalytic materials for photo- and thermo-driven hydrogen production and hydrogenation reactions.

Jun Ma

Jun Ma received his B.S. degree in material chemistry in 2016 and Ph.D. in inorganic chemistry in 2021 under the supervision of Professor Yujie Xiong, both from the University of Science and Technology of China. His research interest is focused on the controlled synthesis of oxide materials and photocatalytic C–H bond activation.

oriented Bi oxyhalide (*i.e.* BiOX, X = Cl, Br or I) electrocatalyst to produce formic acid from CO_2 in a flow cell. They found that the bromide activated bismuth catalyst can achieve a high current density (>100 mA cm^{-2}) and formic acid selectivity (>90%), thus paving the way for the rational design of excellent electrocatalysts for renewable chemical and fuel production.[9] In addition, Su *et al.* employed monodisperse cobalt phthalocyanine (CoPc) on single-walled CNTs (CoPc/SWCNTs) to catalyze the formation of methanol in a tandem-flow electrolyser, which achieves a methanol partial current density of >90 mA cm^{-2} with >60% selectivity.[11] These great advances are accelerating the industrialization of direct CO_2 utilization technologies, and thus the overall pace of carbon neutrality. However, formic acid and methanol can also be obtained in quantity from traditional chemical routes such as petroleum and biomass,[15–17] which leads to a temporary oversupply of these two chemicals (Scheme 1). Therefore, how to use them *via* an efficient and green route will be a dilemma for the future society.

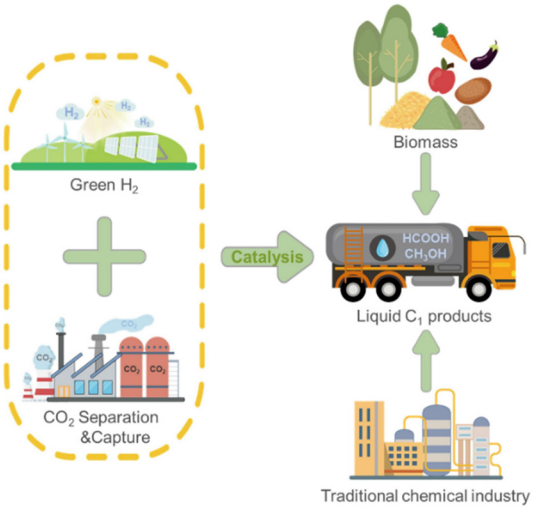

Scheme 1 Main synthetic paths of formic acid and methanol.

In this review, we therefore propose that formic acid and methanol can be the ideal hydrogen sources to replace high pressure H_2 in hydrogenation reactions. Hydrogenation is one of the most critical and fundamental processes in the modern chemical industry, and can produce important chemical and pharmaceutical intermediates.[18–23] However, the use of high pressure hydrogen inevitably leads to some disadvantages such as safety, storage and transportation, and the selectivity of the desired product is difficult to control.[24–27] In this respect, the catalytic transfer hydrogenation using organic hydrogen donors is therefore considered as a good alternative to H_2 hydrogenation, which not only reduces the requirements of special equipment but also improves the desired product selectivity due to the diversity of organic hydrogen donors (Scheme 2). In recent years, some progress has been made in catalytic transfer hydrogenation.[21,23,24,28–33] For example, Gilkey and Xu have reviewed the recent progress in catalytic transfer hydrogenation for the conversion of biomass-derived feedstocks to fuels and chemicals with a focus on mechanistic interpretation, and they also discussed future challenges and opportunities.[34]

Currently, the common hydrogen donors mainly include low molecular mass alcohols (*e.g.*, methanol, ethanol, and isopropanol), and formic acid is also an ideal hydrogen storage medium with a high hydrogen content of 4.4 wt% and stable chemical properties.[35–40] Recently, Zhai *et al.* reviewed the developments in CO_2 hydrogenation to formic acid/formate and reverse formic acid/formate dehydrogenation as a liquid organic hydrogen donor under mild conditions.[41] Such a CO_2–formic acid hydrogenation cycle not only promotes CO_2 capture and utilization, but also provides great guidance for the subsequent hydrogen-related energy and chemical industry. Considering that the CO_2 hydrogenation to formic acid has been discussed by many researchers,[8,9] here we focus only on the progress in transfer hydrogenation using formic acid as

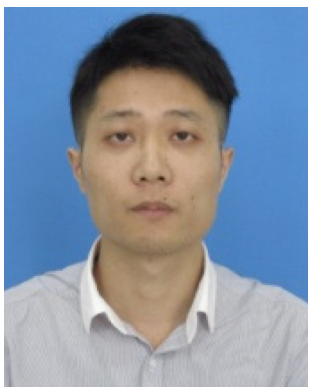

Wanbing Gong

Wanbing Gong received his PhD degree from the University of Science and Technology of China in 2018 under the supervision of Professor Huijun Zhao. Then, he joined the Hefei Institutes of Physical Science, Chinese Academy of Sciences as a postdoc. He is currently a research associate professor at the University of Science and Technology of China. His current research interests focus on searching for new nonprecious catalytic materials and novel catalytic systems to meet the need of industries.

Ran Long

Ran Long received her BSc degree in chemistry in 2009 and PhD in inorganic chemistry under the tutelage of Professor Yujie Xiong in 2014, both from the University of Science and Technology of China. After postdoctoral training with Professors Yujie Xiong and Li Song, she is currently a professor working at the USTC. Her research interests focus on the controlled synthesis and catalytic applications of metal nanocrystals.

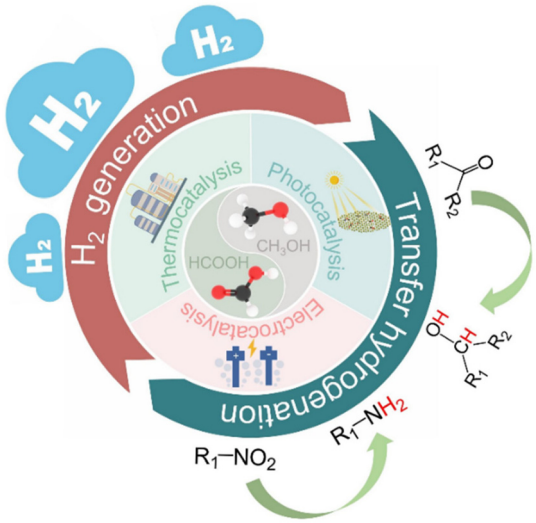

Scheme 2 Proposed transfer hydrogenation process using formic acid and methanol as hydrogen sources.

the hydrogen source, especially in terms of catalysts. In the past few decades, researchers have devoted much effort to developing highly efficient homogeneous and heterogeneous catalysts for the dissociation of formic acid into H_2 and subsequent hydrogenation.[15,38,42–48] Homogeneous catalysts are mainly transition metal–organic complexes, including ruthenium, iridium, nickel, *etc.*, which usually have high activity and good selectivity.[49–51] Compared with homogeneous catalysts, heterogeneous catalysts are easy to separate from the reaction and can be recycled.[52] At present, heterogeneous catalysts used for formic acid transfer hydrogenation are mainly divided into supported precious metal (*e.g.*, Pd, Pt, Au, and Ag) catalysts[53–55] and carbon coated transition metal (*e.g.*, Co, Ni, and Fe) catalysts.[25,56–58] Precious metals usually have high catalytic activity and stability in corrosive formic acid solution, but their scarcity and high price limit their further development.[25,57–59] Fortunately, the low activity and poor stability of transition metals are being gradually overcome *via* carbon coating, which can efficiently inhibit the direct contact between nonprecious nanoparticles (NPs) and formic acid.[57,58,60–62] Moreover, the electron transfer between the coated carbon layer and the metal NPs endows it with excellent catalytic activity to accelerate formic acid adsorption and subsequent dissociation. Compared with direct H_2 hydrogenation, formic acid-driven transfer hydrogenation can not only hydrogenate specific functional groups, but also trigger a series of reactions such as the methylation of aromatic amines using the abundant reaction sites of formic acid itself.[33,63–66]

As another liquid hydrogen source, methanol is also an ideal substitute for high pressure hydrogen.[67–71] Currently, traditional thermocatalysis and electrocatalysis systems have exhibited great potential for the production of methanol on a larger scale, but efficient use of excessive methanol remains a headache in the future chemical industry. Industrially, methanol can be used for producing basic building blocks such as ethylene or propylene, and can also be used as a gasoline additive.[72–77] More importantly, methanol has been regarded as an ideal liquid hydrogen source due to its high hydrogen capacity of 12.5 wt%.[37,39,71] However, it is rarely used for transfer hydrogenation due to high energy consumption for *in situ* hydrogen production and utilization. There are four primary routes for hydrogen production from the traditional thermal catalytic process: methanol steam reforming (MSR),[78–80] methanol decomposition (MD),[81,82] partial oxidation of methanol (POM),[83,84] and a combination of oxidative methanol steam reforming (OMSR, MSR, and POM), also known as autothermal reforming of methanol (ATRM).[85–87] The main approach for producing hydrogen at present is methanol steam reforming ($CH_3OH + H_2O \rightarrow CO_2 + 3H_2$). However, this process is energy-intensive, demanding specific temperature and pressure conditions, thus leading to substantial fossil energy consumption and the generation of carbon dioxide as a by-product. This is not conducive to environmentally friendly sustainable development. While Lin *et al.* have reported that platinum (Pt) atoms dispersed on α-molybdenum carbide (α-MoC) can achieve an outstanding low-temperature MSR performance, significantly increasing the H_2 generation rate and minimizing fossil energy consumption in MSR reactions,[69] the reliance on precious metal catalysts like Pt, Pd, and Ru remains unavoidable.[88] This poses challenges for practical implementation in industrial production.

Compared to thermal catalysis, electro-reforming of methanol, also known as methanol–water co-electrolysis, presents a compelling alternative to traditional reforming methods.[89] This is because it employs an indirect methanol oxidation reaction (MOR) to replace the sluggish oxygen evolution reaction (OER), thereby effectively accelerating the hydrogen production rate of the cathodic hydrogen evolution reaction (HER).[90–92] Additionally, this process transforms methanol

Yujie Xiong

Yujie Xiong received his B.S. degree in chemical physics in 2000 and Ph.D. in inorganic chemistry in 2004, both from the University of Science and Technology of China. During 2004–2009, he worked as a postdoc at the University of Washington in Seattle and as a research associate at the University of Illinois at Urbana-Champaign, respectively. He was a principal scientist of the National Nanotechnology Infrastructure Network (NSF-NNIN) site at Washington University in St Louis in 2009–2011. He joined the USTC in 2011, and currently is the chair professor of chemistry. His research centers on artificial cycles of elements and energy toward ecosystem reconstruction.

into some high-value byproducts instead of CO_2 or CO. Moreover, the energy input for electrocatalytic methanol reforming is significantly lower than that required for complete decomposition of water and thermal catalytic methanol reforming. This aspect holds great significance for reducing the overall energy consumption.[93,94] For instance, Guo *et al.* developed a bi-functional co-doped Rh electrocatalyst, where an enhanced HER on the cathode was coupled with an accelerated MOR on the anode. This design achieved an efficient rate for complete hydrogen decomposition and provided an impressive mass activity of up to 889 mA mg^{-1} for the MOR.[95]

Simultaneously, given solar energy's status as a high-quality sustainable resource, attention has shifted towards driving methanol steam reforming (MSR) through light and the exploration of nonprecious metal catalysts.[96–99] Li *et al.* successfully prepared a novel L–Cu catalyst for photo-driven MSR by reducing CuAl layered double hydroxide (CuAl-LDH) nanosheets, demonstrating an exceptional hydrogen production activity of 160.5 μmol g_{cat}^{-1} s^{-1}.[100] Despite substantial efforts to improve the H_2 production rate in MSR reactions, there has been limited focus on investigating carbon-containing by-products. The predominant emphasis in most studies has been on reducing CO production. This emphasis is driven by the imperative to prevent CO poisoning of precious metal catalysts,[101] a factor detrimental to the application of proton exchange membrane fuel cells (PEMFC), which mandate CO concentrations below 10 ppm at the anode.[102] Unfortunately, the potential utilization of carbon-containing products derived from semi-oxidation reactions is frequently overlooked, leading to significant resource wastage. Therefore, achieving efficient hydrogen production and highly selective generation of valuable carbon-containing products through light-driven methanol under mild conditions holds substantial practical significance. Tang's group recently developed an environmentally friendly methanol photocatalytic hydrogen production system that harnesses the synergy between Cu single atoms and Pt nanodots on a PtCu–TiO_2 catalyst. The results showcase a remarkable H_2 formation rate of 2383.9 μmol h^{-1}, an apparent quantum efficiency reaching 99.2%, and the high-value carbon-containing product, formaldehyde, with a selectivity of up to 98.6%.[103] Additionally, Wang's group engineered single-atom rhodium-doped metal sulfide nanorods, featuring alternately stacked wurtzite/zinc blende segments. The design efficiently activated the methanol C–H bond to generate hydrogen under light, yielding ethylene glycol at a rate of 34 mmol g_{cat}^{-1} h^{-1}, maintaining a consistent selectivity of approximately 85%.[104] These examples illustrate significant advancements in methanol hydrogen production, underscoring the substantial application potential of clean and efficient photocatalysis and electrocatalysis in this domain. Such progress can effectively propel the seamless integration of subsequent hydrogen production and hydrogenation processes. It also encourages the advancement of transfer hydrogenation reactions using methanol as a hydrogen source, paving the way for crucial breakthroughs in the future.

In the past few years, much research has been done on the hydrogen production and hydrogenation systems of formic acid and methanol; however, few reviews have focused on the transfer hydrogenation reactions using CO_2-derived methanol and formic acid as hydrogen sources, let alone catalytic material design. In this review, we first summarize the developments of catalysts in the transfer hydrogenation process (*e.g.*, thermal catalysis and photocatalysis) using formic acid as a hydrogen source, mainly including Pd-based precious metal catalysts and Co-based nonprecious metal catalysts. Similarly, we also analyze the catalyst design strategies for methanol-driven transfer hydrogenation reactions, and Pd-based and Cu-based materials are mainly discussed. Finally, in view of the current developments of catalysts in this field, we propose some key challenges and corresponding opportunities for transfer hydrogenation.

2. Transfer hydrogenation using formic acid as a hydrogen source

2.1. Catalyst design for the thermocatalytic process

Thermocatalytic hydrogenation using formic acid as a hydrogen source is one of the fundamental processes in modern chemical industries.[45,56] In theory, two kinetic pathways may occur when formic acid is used as a hydrogen source: (i) dehydrogenation of formic acid to form H_2 and CO_2 (dehydrogenation pathway) and (ii) dehydration of formic acid to form H_2O and CO (dehydration pathway). The latter is undesired because the dehydration pathway will not only result in a decrease in the concentration of hydrogen, but also produce by-product CO, leading to the poisoning of heterogeneous catalysts (Scheme 3).[15,38,47,62,105,106] Currently, thermo-catalytic hydrogenation using formic acid as a hydrogen source usually requires harsh reaction conditions (high temperature or long time) and highly efficient catalysts.[56] For example, the strong corrosive properties of formic acid hamper the long-term stability of catalysts.[61,62] Therefore, it is necessary to summarize the recent progress in catalyst development for thermocatalytic hydrogenation using formic acid as a hydrogen source.

2.1.1. Precious metal-based heterogeneous catalysts

Palladium-based NP catalysts. Among all the precious metal catalysts, Pd based catalysts are the most effective and thus

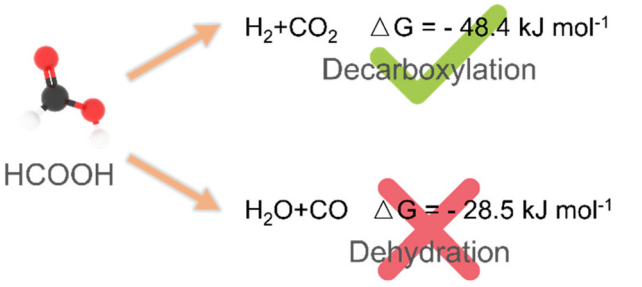

Scheme 3 The possible routes for formic acid decomposition.

widely studied candidates because of their special electronic structures and adsorption patterns.[107–112] As we all know, the catalytic performance of heterogeneous catalysts greatly depends on their support;[113–118] we therefore categorize and summarize the recent developments of Pd catalysts for the hydrogenation reactions using formic acid as a hydrogen source according to the type of support.

First of all, carbon materials have been regarded as a typical catalyst support for formic acid transfer hydrogenation because of their large surface area, high porosity, easy modification, strong chemical stability, *etc.*[119–123] In particular, heteroatoms such as N or S doped carbon supports have obvious electronic effects, which leads to excellent formic acid dehydrogenation and subsequent hydrogenation performance.[23,58,124–128]

López Granados *et al.* investigated and found that Pd/C was the most effective and hydrogenation of hydromaleic acid identified specific active sites to succinic acid using formic acid as a hydrogen source for different combinations of precious metals (Pd, Au, Ru, Pt, and Rh) and supports (γ-Al_2O_3, TiO_2, CeO_2, ZrO_2, WO_3, $CeZrO_4$, C, Nicanite, SiO_2 and TS-1).[55] Zhang *et al.* also found that the hydrogenation activity followed the trend of Pd/activated carbon (AC) > Pd/TiO_2-AC > Pd/MIL-101 > Pd/TiO_2 > Pd/Al_2O_3 for the catalytic transfer hydrogenation of phenol to cyclohexanone, and the optimum Pd/AC catalyst can be recycled at least 6 times. The effect of formic acid on the hydrogenation activity of supported Pd catalysts was also studied. For the MIL-101 and oxide (TiO_2 and Al_2O_3) supports, they revealed that the low activity may be due to the competitive adsorption of formic acid with phenol at a single Pd site (Fig. 1a).[129] Afterwards, heteroatoms such as N- or S-doped carbon supported Pd catalysts were further studied. Hu *et al.* showed that nitrogen functionalized carbon nanotube supported Pd NPs (Pd/NCNT) were especially suitable for the transfer hydrogenation of phenol using formic acid as a hydrogen donor, compared to oxygen functionalized Pd/OCNT (Fig. 1b).[130] For the transfer hydrogenation of Lindane using formic acid as a hydrogen source, Yang *et al.* found that the pyridine N doped porous carbon supported Pd catalyst exhibited good catalytic activity due to the promotional effect of pyridine N, which enhanced the Pd NP dispersion and thus formic acid decomposition. Compared with the commercial bare carbon-supported Pd catalyst, this catalyst can obtain a 99.7% conversion and 100% dechlorination selectivity at 25 °C under atmospheric pressure.[135] For this, Zhang *et al.* prepared ultrafine Pd NPs anchored on N-doped carbon (Pd/N-XC72R), where N-XC72R was prepared by annealing commercial Vulcan XC72R with urea in advance. They showed that N doping on the carbon surface can significantly enhance the affinity between metal NPs and the support, and avoid the aggregation and over-growth of NPs. Compared with the bare Vulcan XC72R supported Pd catalyst, the prepared Pd/N-XC72R catalyst exhibited better catalytic activity for the transfer hydrogenation of nitroaromatic hydrocarbons at room temperature (Fig. 1c).[131] In addition, graphitized carbon nitride (g-C_3N_4) containing nitrogen is a potential nitrogen-doped carbon material, which has been gradually applied to perform transfer hydrogenation. For example, Xu *et al.* found that the 5 wt% Pd/g-C_3N_4 catalyst can completely convert nitrobenzene to aniline using formic acid as the hydrogen donor and water as the solvent at room temperature. Meanwhile, the Pd/g-C_3N_4 catalyst also had good activity in the one-pot reductive amination of carbonyl compounds and nitro compounds, and the corresponding secondary amines can be obtained with excellent selectivity (>90%) (Fig. 1d).[132] Cheng *et al.* also prepared a Pd@g-C_3N_4 nanosheet catalyst by a liquid-phase exfoliation method for the transfer hydrogenation of nitroaromatic hydrocarbons. The superior activity and stability can be attributed to the amphiphilic g-C_3N_4 support, the uniform dispersion of Pd NPs and the Mott–Schottky effect between g-C_3N_4 and Pd NPs (Fig. 1e).[133] Chou *et al.* prepared the bulk- and nanoflake-g-C_3N_4 supported Pd NP catalysts (Pd/b-CN and Pd/ns-CN) for the catalytic transfer hydrogenation of furfural alcohol to tetrahydrofurfuryl alcohol. The characterization analysis showed that Pd/ns-CN had a higher specific surface area, more surface

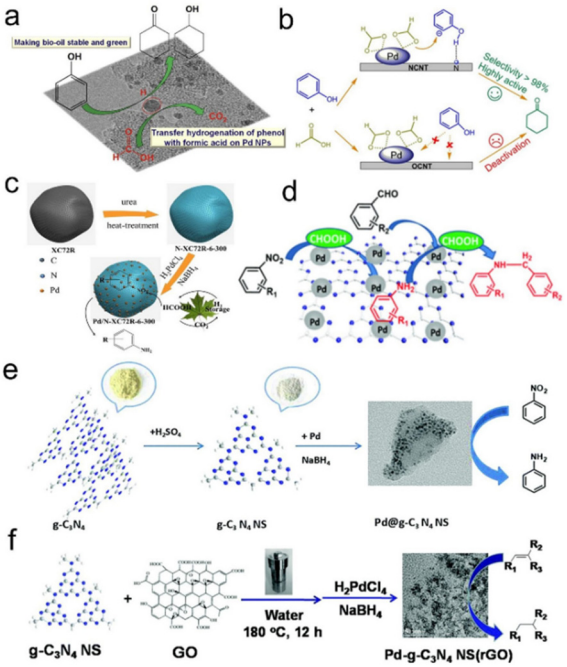

Fig. 1 (a) Schematic illustration of the transfer hydrogenation of phenol on supported Pd catalysts. Reproduced with permission from ref. 129. Copyright 2014 Elsevier. (b) Schematic illustration of different reaction paths on Pd/OCNT and Pd/NCNT. Reproduced with permission from ref. 130. Copyright 2021 Wiley-VCH. (c) Schematic illustration of the preparation progress of Pd/N-XC72R. Reproduced with permission from ref. 131. Copyright 2018 American Chemical Society. (d) Schematic illustration for the preparation of primary and secondary amines over g-C_3N_4 supported Pd NPs. Reproduced with permission from ref. 132. Copyright 2018 Royal Society of Chemistry. (e) Schematic illustration of the preparation process of the Pd@g-C_3N_4 NS catalyst. Reproduced with permission from ref. 133. Copyright 2018 Royal Society of Chemistry. (f) Schematic illustration of the preparation process of the Pd-g-C_3N_4 NS/rGO catalyst. Reproduced with permission from ref. 134. Copyright 2018 Royal Society of Chemistry.

bases and higher Pd dispersion than Pd/b-CN, which are the key factors for the activation of formic acid.[136] Li *et al.* further synthesized porous g-C_3N_4 nanosheets/reduced graphene oxide composites by hydrothermal co-assembly of graphene oxide and g-C_3N_4 nanosheets. Owing to the synergistic support effects, the obtained Pd catalyst showed significant catalytic activity for olefin hydrogenation with formic acid and formates as hydrogen sources under atmospheric pressure (Fig. 1f).[134]

In addition to carbon materials, other supports were also studied. For instance, Zhang *et al.* synthesized a layered Ti_3C_2 MXene supported Pd NP catalyst, which could achieve efficient and selective hydrogenation of nitrobenzene in the presence of formic acid. They confirmed that the electron-deficient Pd NPs regulated the reaction pathway and promoted the dissociation of formic acid, thus improving the production of active H* to hydrogenate nitrobenzene.[137] Neeli *et al.* synthesized Pd NPs with an average diameter of 2.2 nm by anion exchange and chemical reduction on NH_2-UiO-66. The as-prepared Pd/NH_2-UiO-66 catalyst can catalyze the transfer hydrogenation of nitrobenzene to aniline in mild water with formic acid as a hydrogen source, and the excellent catalytic activity was mainly attributed to the synergistic effect of Pd NPs and NH_2-UiO-66 (Fig. 2a).[138] For the unsupported Pd catalysts, our group identified specific active sites (*i.e.*, surfaces, corners and edges) for formic acid decomposition and olefin/nitrobenzene hydrogenation. The results showed that the decomposition of formic acid mainly occurs at the edge of cubic nanocrystals and the plane of octahedral/tetrahedral nanocrystals, and hydrogenation mainly occurs at the edge of cubic and octahedral/tetrahedral nanocrystals.[140]

In addition to single metal sites, Pd-based bimetallic catalysts usually exhibit strong catalytic properties due to the electronic and geometric synergistic effects of bimetallic sites. Liu *et al.* prepared Pd–Ag bimetallic NPs on N-doped porous carbon by using one-step doped NH_2-MIL-125 as the precursor. Due to the synergistic interaction between the support and Pd-Ag bimetallic NPs, the as-synthesized Pd_9Ag_1-N-doped-MOF-C catalyst exhibited excellent catalytic activity and selectivity for the catalytic transfer hydrogenation of nitroaromatics using formic acid as a renewable hydrogen donor (Fig. 2b).[139] Cui *et al.* first prepared mesoporous N-doped carbon supported Ni NPs (Ni/mCN) through pyrolysis of a mixture of polyacrylonitrile, melamine and $Ni(NO_3)_2{\cdot}6H_2O$. Then, Ni/mCN was treated with $Pd(AcO)_2$ to form a PdNi bimetallic NP catalyst (PdNi/mCN). The as-prepared PdNi/mCN catalysts showed higher catalytic activity at room temperature for the transfer hydrogenation of nitroarenes using formic acid as a reducing agent, which may be due to the high dispersion of PdNi bimetallic NPs, the maximum utilization rate of Pd atoms and the special structure of mesoporous N-doped carbon (Fig. 2c).[54]

Other precious metal-based NP catalysts. In addition to Pd-based catalysts, other precious metal materials have also been studied and they exhibited excellent catalytic performance. Li *et al.* developed a simple and reliable process for the selective transfer hydrogenation of semi-reduced alkynes using formic acid as a hydrogen source and supported Au as a catalyst, which exhibited high activity, selectivity and recyclability under mild reaction conditions (Fig. 3a).[141] Furthermore, Zhang *et al.* developed a TiO_2-supported Au catalyst coated with an N-doped porous carbon layer using a polydopamine-coating-carbonization strategy. For the conversion of 5-hydroxymethylfurfural to 5-methylfurfural, the obtained Au/TiO_2@NPC showed high catalytic performance with a >95% 5-methylfurfural yield. The experimental results showed that the catalytic performance was related to the suitable combination of highly dispersed Au NPs in the core–shell nanostructure and good interfacial interaction (Fig. 3b).[142]

Besides, Neeli *et al.* synthesized the Rh/ED-KIT-6 catalyst with an average particle size of 1.2 nm by chemical reduction of the Rh^{3+} precursor on KIT-6. The synergistic effect of the nitrogen function and ultrafine Rh NPs endowed it with excellent catalytic activity for transfer hydrogenation of furfural to furfuryl alcohol with formic acid as a hydrogen source without other additives (Fig. 3c).[143] Zhou *et al.* used formic acid as the only hydrogen resource to selectively synthesize γ-valerolactone

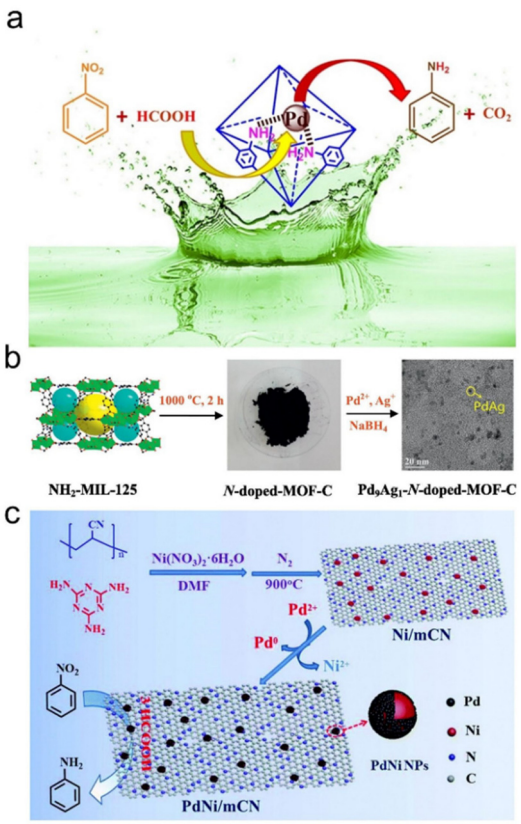

Fig. 2 (a) Schematic illustration of the transfer hydrogenation of nitrobenzene on Pd nanoparticles supported on NH_2-UiO-66. Reproduced and modified with permission from ref. 138. Copyright 2018 Elsevier. (b) Schematic illustration of the preparation progress of Pd_9Ag_1-N-doped-MOF-C. Reproduced with permission from ref. 139. Copyright 2017 Elsevier. (c) The preparation procedure and application of the PdNi/mCN nanocatalyst. Reproduced with permission from ref. 54. Copyright 2018 Royal Society of Chemistry.

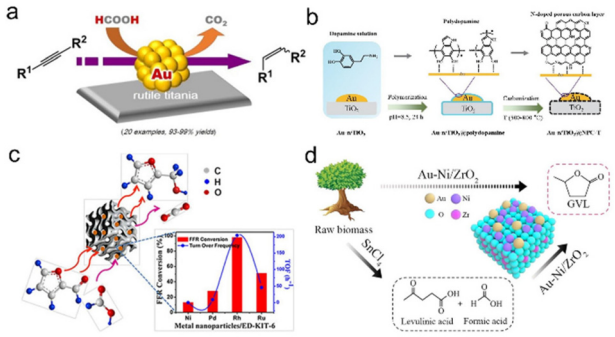

Fig. 3 (a) Heterogeneous gold-catalyzed selective semireduction of alkynes. Reproduced with permission from ref. 141. Copyright 2016 Wiley-VCH. (b) Schematic illustration of the synthesis procedure of Au-n/TiO_2@NPC-T. Reproduced with permission from ref. 142. Copyright 2022 Elsevier. (c) Ultrasmall Rh nanoparticles embedded on diamine-functionalized KIT-6. Reproduced with permission from ref. 143. Copyright 2017 Wiley-VCH. (d) γ-Valerolactone production from furfural *via* an integrated strategy on Au–Ni/ZrO_2. Reproduced with permission from ref. 144. Copyright 2020 American Chemical Society.

from raw lignocellulosic biomass. The first step used $SnCl_4$ as the catalyst to prepare levulinic acid and formic acid, and the second step used the developed Au-Ni/ZrO_2 bimetallic catalyst to produce γ-valerolactone from levulinic acid. Compared to the Au/ZrO_2 catalyst, an appropriate Ni loading amount can promote the reduction of $Au^{\delta+}$ to Au^0 and the dispersion of Au^0 without aggregation, which can increase the hydrogenation reaction and the subsequent dehydration reaction (Fig. 3d).[144]

2.1.2. Nonprecious metal-based heterogeneous catalysts

Cobalt-based NP catalysts. The high price and scarcity of precious metal catalysts limit their industrial application, which urgently requires efficient design and precise preparation of nonprecious metals. However, nonprecious metal catalysts still face some challenges such as low activity and poor stability, and harsh reaction conditions such as high temperature inevitably increase overall energy consumption.[40,128,145–148] Moreover, strong corrosion of formic acid also put forward a big challenge to improve the stability of nonprecious metal catalysts for hydrogenation reactions.

The carbon supported or coated Co catalysts were therefore used as highly efficient transfer hydrogenation samples when using formic acid as a hydrogen source. Beller's group pioneerly prepared cobalt oxide based catalyst (Co_3O_4-NGr@C) by pyrolysis of the cobalt–phenanthroline complex on commercial Vulcan XC72R. It achieved excellent performance for the transfer hydrogenation of nitroaromatics, olefins, aldehydes, ketones, esters, amides and nitriles. They also prepared a carbon supported nitrogen-modified cobalt catalyst by pyrolyzing a mixture of $Co(AcO)_2$ in melamine or waste melamine resin solutions. The selective transfer hydrogenation of *N*-isoaromatic hydrocarbons can be achieved with formic acid as a hydrogen source and ethanol as the solvent. At the same time, this nonprecious Co catalyst also showed certain activity and selectivity of formic acid dehydrogenation (Fig. 4a).[57,60] As far as carbon sources are concerned, melamine is a cheap and readily available carbon source and contains nitrogen species. Yuan *et al.* prepared the N-doped carbon coated Co NP catalyst (Co@NC) by using melamine and $Co(AcO)_2$ through hydrothermal and carbonization treatment, this structure effectively avoided the corrosion and leaching of Co NPs. As a result, Co@NC greatly promoted the catalytic transfer hydrogenation of various functionalized nitroaromatic hydrocarbons with formic acid as a hydrogen donor in water/ethanol solution without alkali (Fig. 4b).[61] Kar *et al.* prepared a porous N-doped carbon coated cobalt catalyst (Co@C-N800) using *o*-phenylenediamine (OPD) as C and N sources and melamine as

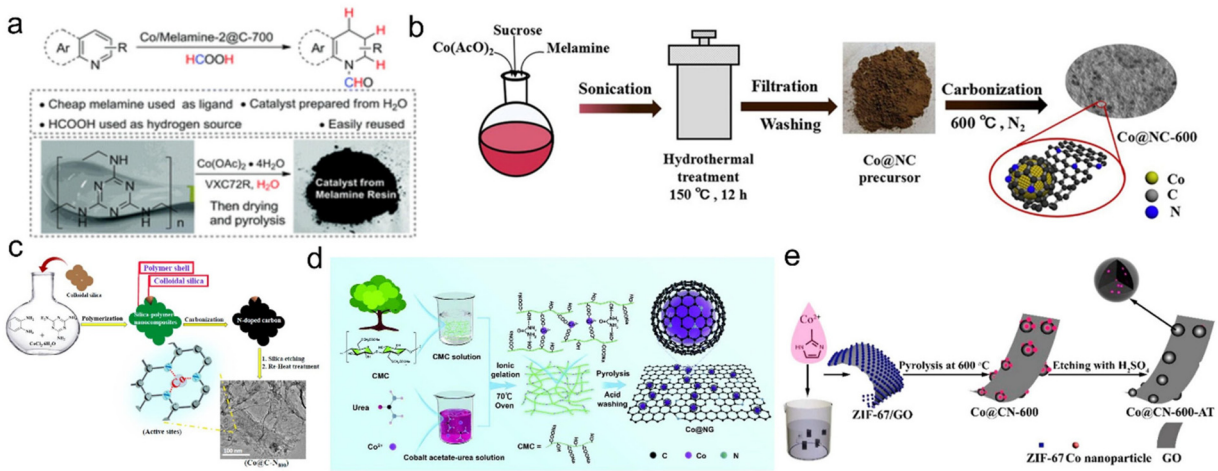

Fig. 4 (a) Preparation of cobalt nanoparticles from melamine in water. Reproduced with permission from ref. 60. Copyright 2017 Royal Society of Chemistry. (b) Preparation of Co@NC catalysts. Reproduced with permission from ref. 61. Copyright 2018 Wiley-VCH. (c) Stepwise synthesis protocol adopted for the preparation of Co@C–N_x materials. Reproduced with permission from ref. 62. Copyright 2019 American Chemical Society. (d) The fabrication process of Co@NG. Reproduced with permission from ref. 149. Copyright 2019 Royal Society of Chemistry. (e) Schematic illustration of the synthesis of the Co@CN-600-AT catalyst. Reproduced with permission from ref. 150. Copyright 2017 American Chemical Society.

additional N sources. Using formic acid as a hydrogen source, this catalyst achieved 92.1% quinoline conversion and 87% selectivity for 1,2,3,4-tetrahydroquinoline (Fig. 4c).[62] Additionally, Zhou *et al.* prepared a multilayer N-doped graphene catalyst with highly dispersed cobalt NPs (Co@NG) using carboxymethyl cellulose as the raw material. Using urea as a non-corrosive activator can introduce porous strip nanostructures and abundant nitrogen. With formic acid as a hydrogen source, alkaline transfer hydrodeoxygenation can be realized with a 99% 2-methoxy-*p*-cresol yield on optimized Co@NG-6 with the highest proportion of pyridine-N. The superior catalytic performance can be attributed to the synergistic effect of the strong interaction between doped N atoms and coated Co NPs. Deuterium kinetic isotope experiments showed that protic $N–H^+$ and hydrogenated $Co–H^-$ were two active intermediates. Finally, the graphene shell prevented the corrosion and aggregation of Co NPs under real reaction conditions (Fig. 4d).[149] Cobalt-containing metal–organic frameworks (MOFs) such as ZIF-67 are often used as cobalt and carbon sources. For example, Jiang *et al.* used the ZIF-67/GO composite by depositing ZIF-67 on the GO layer to prepare the N-doped carbon-based cobalt catalyst. The transfer hydrogenation reaction can be performed on this catalyst using formic acid as a hydrogen donor and tetrahydrofuran as the solvent. The structurally diverse secondary amines were produced with excellent yields without reducing other functional groups (Fig. 4e).[150]

The morphology and structure of carbon materials are also very important for catalytic hydrogenation performance. Xu *et al.* prepared Co NPs coated with the N-doped carbon nanotube catalyst (Co@NCNTs-800) through multiple pyrolyses of dicyandiamide and cobalt(II) acetylacetone. The outer nitrogen-doped carbon nanotubes can prevent the agglomeration and leaching of the enclosed Co NPs, and the defects formed by N doping were beneficial for embedding active molecules on the surface of Co NPs (Fig. 5a).[151] Besides, some researchers have done much investigations about the N and S co-doped carbon supported Co materials. Zhu *et al.* prepared Co NPs coated with N and S co-doped carbon nanotubes by one-pot pyrolysis of melamine, thiocyanic acid and cobalt nitrate hexahydrate. The corrosion, leaching and agglomeration of Co NPs could be effectively avoided by double-heteroatomic co-doped porous carbon materials. They found that the synergistic interaction between Co NPs and N,S atoms can promote the ability of transfer hydrogenation and formylation of nitroaromatic hydrocarbons, especially the incorporation of S atom greatly improved the selectivity of the *N*-formylation reaction (Fig. 5b).[152] In addition, Chen's group first synthesized an organic precursor (POPs) through the solvothermal condensation of melamine and terephthalic acid in dimethyl sulfoxide. Then pyrolysis of POPs impregnated with cobalt nitrate was used to successfully embed Co in a porous carbon catalyst with N,S co-doping. The catalyst can be used for the hydrogen-

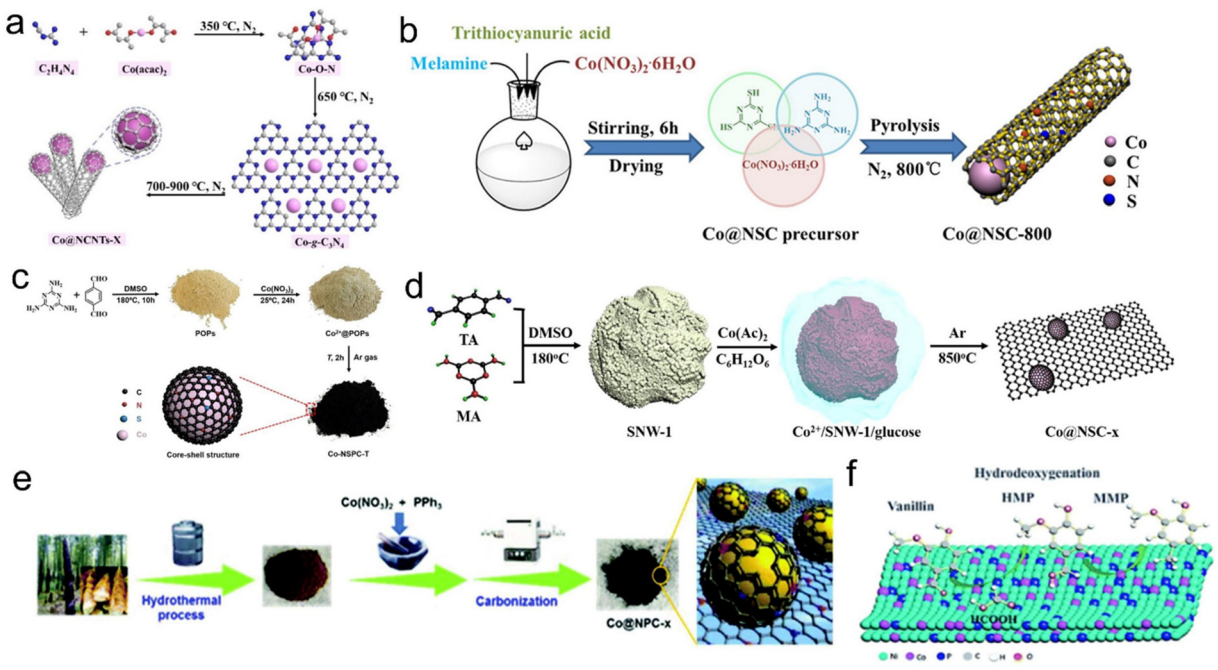

Fig. 5 (a) Schematic of the synthesis process of Co@NCNTs-*X*. Reproduced with permission from ref. 151. Copyright 2019 Wiley-VCH. (b) Preparation process of the Co@NSC-800 catalyst. Reproduced with permission from ref. 152. Copyright 2020 American Chemical Society. (c) The fabrication of the Co-NSPC-T catalysts. Reproduced with permission from ref. 153. Copyright 2018 Wiley-VCH. (d) Diagram for the fabrication of Co@NSC-*x*. Reproduced and modified with permission from ref. 127. Copyright 2019 American Chemical Society. (e) Schematic illustration of the preparation of Co NPs coated with an N,P-codoped carbon shell. Reproduced with permission from ref. 58. Copyright 2018 Royal Society of Chemistry. (f) *In situ* hydrodeoxygenation of vanillin over Ni–Co–P/HAP. Reproduced with permission from ref. 154. Copyright 2021 Royal Society of Chemistry.

ation of nitrobenzene to aniline with formic acid as a hydrogen source without alkali. In their experiments, Co NPs were confirmed as the active sites of the reaction, and their electron transfer to the carbon shell was crucial to the hydrogenation performance. The incorporation of the S heteroatom in the N-doped carbon layer can improve the electron transfer process and the positive charge of Co, thus improving acid resistance. To further improve the hydrogenation performance of this catalyst, they further prepared N,S co-doped carbon embedded with Co NPs (1.14 wt%) by pyrolyzing the complex of the Schiff-base network (SNW-1) and $Co(Ac)_2$ coated with glucose. It can be seen that the glucose coating prevented highly dispersed Co NPs from directly bonding with S species. Consequently, the catalyst showed excellent catalytic activity and stability for the catalytic transfer hydrogenation using formic acid as a hydrogen source in the alkali-free system, and thus generated multiple secondary amines with excellent yields through hydrogenation and reducing amination domino aggregate reaction (Fig. 5c and d).[127,153] In addition to N,S co-doped carbon, Duan *et al.* developed N,P co-doped carbon coated Co NPs (Co@NPC-800) using cheap and easily available PPh_3 as the P source *via* a simple and green synthesis method. When N and P were uniformly added to the carbon lattice, they showed that the functionalized nitroaromatics can be efficiently and selectively hydrogenated to the corresponding aniline under the condition of formic acid or ammonium formate as the hydrogen donor and tetrahydrofuran/water as the solvent (Fig. 5e).[58] In addition to monometallic sites, bimetallic sites have also received some attention and developments. Duan *et al.* synthesized a novel Ni–Co–P/HAP amorphous alloy catalyst by the impregnation–reduction method, and achieved a high yield of 2-methoxy-4-methylphenol by hydrodeoxygenation of vanillin using formic acid as a hydrogen source and isopropyl alcohol as the solvent. They revealed that the Co site can increase the disorder of Ni-based amorphous alloy and reduce the agglomeration of the catalyst (Fig. 5f).[154] Zhao *et al.* prepared a $CoFeO_x$-modified CoFe bimetallic catalyst by high-temperature calcination with Co–Mg–Fe layered dihydroxide as the precursor. Under the condition of formic acid as the hydrogen source, the efficient transfer hydrogenation of 5-hydromethylfurfural to 2,5-dimethylfuran was achieved due to the synergistic interaction between bimetallic CoFe NPs, $CoFeO_x$ species with abundant defects and surface base sites, effectively promote the dehydrogenation of formic acid. Owing to the high degree of alloying, and strong interaction between CoFe NPs and the support, the as-prepared CoFe catalyst also exhibited excellent acid resistance.[155] Yang *et al.* achieved the catalytic transfer hydrogenation of 5-hydroxymethylfurfural to the 2,5-dimethylfuran with a >90% yield on a carbon-supported nickel-cobalt catalyst (Ni–Co/C) using formic acid as a hydrogen donor.[156]

Recently, with the rapid development of single-atomic materials, single-atomic catalysts have demonstrated excellent performance in transfer hydrogenation using formic acid as a hydrogen source. Lu's group used the $Co(phen)_2(OAc)_2$ complex as precursor and SBA-15 as a hard template to prepare an ordered mesoporous N-doped carbon-confined highly dispersed $Co–N_x$ as the catalyst (Co–NC). Compared with direct H_2 hydrogenation, formic acid inhibited the hydrogenation reaction during the formation of 2,5-furandimethyl alcohol. Subsequently, they further developed a cascade catalytic system ($NiCl_2$/FA/Co-NC) to produce 2,5-furandimethanol from glucose and di/polysaccharide in a one-pot reaction (Fig. 6a).[157,158] Han *et al.* successfully used template-assisted pyrolysis to stabilize isolated cobalt single-atomic sites on an ordered porous nitrogen-doped carbon (ISAS-Co/OPNC) using SBA-15 as a sacrificial template. When formic acid or exogenous hydrogen was used as a hydrogen source, both the release of H_2 by N-heterocyclic dehydrogenation and the storage of H_2 by the reverse transfer of N-heterocyclic hydrogenation (or hydrogenation) showed high catalytic activity (Fig. 6b).[59] Huang *et al.* reported that a $Co(acac)_2$ metal precursor was encapsulated in an aerotocan/sodium dodecyl sulfate hydrogel, and S,N co-doped carbon-supported Co single-atomic catalyst (Co/SNC) was synthesized by the microencapsulation pyrolysis method. The transfer hydrogenation of *N*-isoaromatic hydrocarbons was performed with formic acid as a hydrogen donor without acid leaching (Fig. 6c).[159] Gong *et al.* prepared an N-doped carbon based Co catalyst ($Co–N_x$/C-800-AT) by pyrolyzing cobalt phthalocyanine-silica colloidal composite and removing silica templates and Co NPs by pickling, in which cobalt–nitrogen species ($Co–N_x$) was the active site of the reaction. *N*-substituted pyrrole compounds have been synthesized by the heterocyclic reaction of nitrocompounds with 2,5-hexadione using formic acid as a hydrogen source and acid catalyst using the Paal–Knorr shrinkage method (Fig. 6d).[160] Zhang *et al.* proposed a template-assisted spatial restriction strategy for the preparation of ultra-high Co single-atomic sites (10.26 wt%) embedded N-doped graphene-like carbon by one-step pyrolysis. In the presence of formic acid, the optimum Co SSCs@NG-800-50 catalyst exhibited excellent catalytic performance for the transfer hydrogenation of nitrobenzene with a 99% conversion and 96.3% selectivity of aniline. DFT calculations combined with detailed experiments revealed that active H was first generated by the dissociation of the C–H bond in HCOOH rather than the known O–H bond, and then used for hydrogenation of nitroaromatics at the CoN_3 site (Fig. 6e).[161] Li *et al.* prepared cobalt single-atoms anchored on N-doped ultra-thin carbon nanosheets (CoSAs/NCNS) to achieve selective nitroaromatic hydrogenation with formic acid as a hydrogen donor and the turnover frequency (TOF) reached 110.6 h^{-1}. Due to the ultra-thin mesoporous structure, the catalytic activity of CoSAs/NCNS was 20 times higher than that of transition metal Co NPs reported in the literature under similar reaction conditions (Fig. 6f).[162]

Other nonprecious metal-based NP catalysts. In addition to cobalt, other nonprecious metals such as Ni and Cu are also used in formic acid driven transfer hydrogenation reactions. Liu *et al.* prepared Ni/CeO_2 catalysts by loading Ni oxides onto CeO_2 nanorods, and the addition of Ni reduced the reduction temperature of the catalyst, forming the Ni–O–Ce interfacial site. In the hydrogenation of levulinic acid with formic acid as

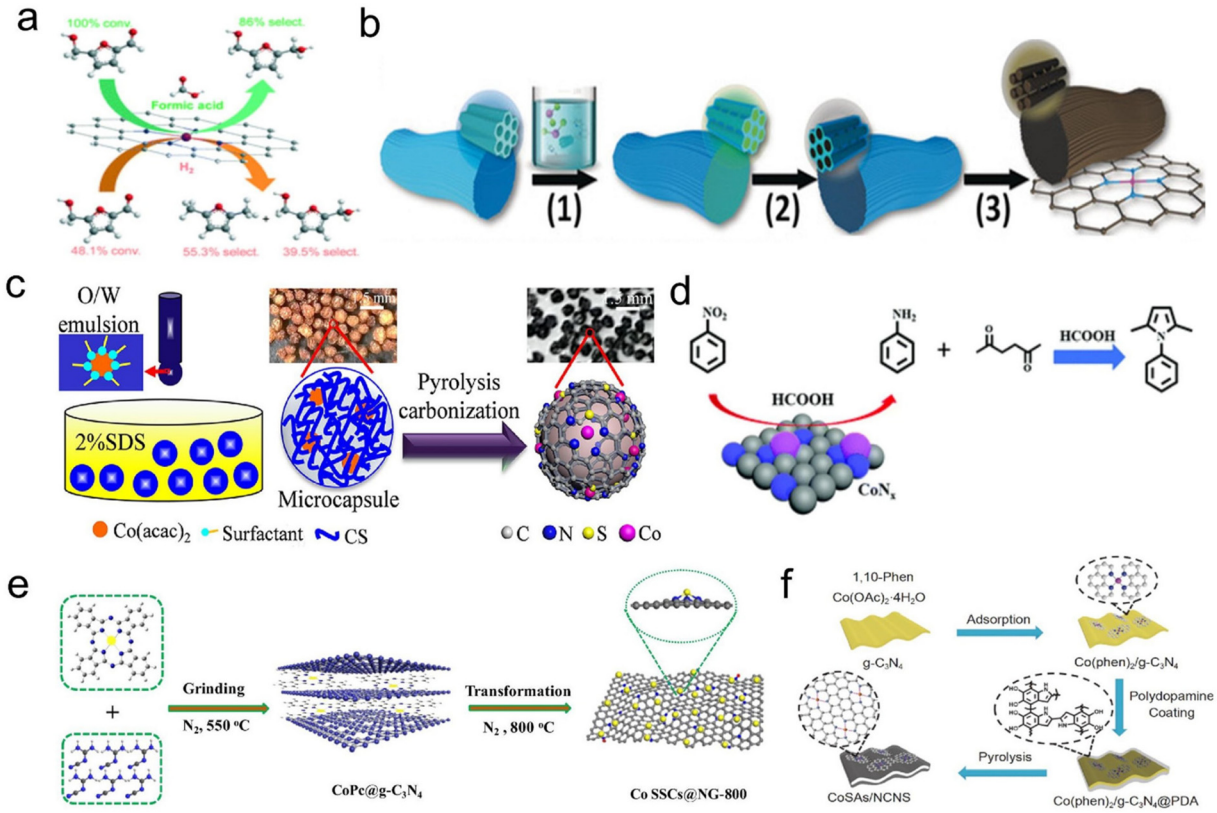

Fig. 6 (a) Schematic illustration of the transfer hydrogenation on highly dispersed Co–N_x sites. Reproduced with permission from ref. 157. Copyright 2021 Royal Society of Chemistry. (b) Illustration of the synthesis of ISAS-Co/OPNC. Reproduced and modified with permission from ref. 59. Copyright 2018 Wiley-VCH. (c) Scheme of the quasi-continuous synthesis of Co/SNC. Reproduced and modified with permission from ref. 159. Copyright 2022 Elsevier. (d) Schematic illustration of the Co–N_x/C-800-AT catalyst. Reproduced with permission from ref. 160. Copyright 2017 Royal Society of Chemistry. (e) Schematic illustration for the preparation of Co SSCs@NC-800. Reproduced and modified with permission from ref. 161. Copyright 2021 Elsevier. (f) Schematic illustration of CoSAs/NCNS preparation. Reproduced with permission from ref. 162. Copyright 2019 Springer Nature.

a hydrogen source, the Ni/CeO_2 catalyst with 6.9 nm particle size and appropriate acidity distribution showed excellent catalytic performance, the conversion of levulinic acid was 73%, and the selectivity of γ-valerolactone was 90%.[163] Wang *et al.* reported *in situ* encapsulation and stabilization of Cu/CuO_x in a porous carbon matrix (Cu/CuO_x@C). Under appropriate reaction conditions, the Cu/CuO_x@C-450 catalyst showed a high furfural conversion of 99.1% with a 98% furfuryl alcohol selectivity due to the high dispersion of Cu/CuO_x NPs and the suitable Cu^0/Cu^{n+} ratio.[164] Lomate *et al.* found the Cu-SiO_2 catalyst showed a higher levulinic acid conversion and valerolactone selectivity when using formic acid as a hydrogen source compared to that of only the SiO_2 support. The key to the high activity and selectivity lies in the strong interaction of some copper oxide monomers with the support and the binding of more acid sites in Cu-SiO_2.[165] Bimetallic synergies also play a nonnegligible role in promoting nonprecious metal based systems. Lin's group investigated the catalytic conversion of 5-formyloxymethylfurfural to 2,5-dimethylfuran over the Ni–Cu bimetallic catalyst using formic acid as a hydrogen donor. They showed that copper was more likely to catalyze the hydrogenation of C–O ester bonds, while nickel species played a dual role in catalyzing the hydrogenation of C–O ester bonds and the hydrodehydration of hydroxyl groups in furan rings. They also developed a Cu–Cs bimetallic catalyst for the catalytic transfer hydrogenation of furfural to furfuryl alcohol. The Cu in CuCs-MCM had the dual function of catalyzing the decomposition of formic acid into hydrogen and hydrogenating furfural into furfuryl alcohol. Meanwhile, the doping of Cs decreased the size of Cu NPs and improved the dispersion of Cu active sites. As an accelerator, Ce played a good role in improving hydrogenation activity by regulating the surface acidity of Cu to an appropriate level (Fig. 7a and b).[166,167]

The stability of nonprecious metal NPs in the formic acid system has always been a big problem, but the appearance of single-atomic catalysts can not only solve the stability problem but also improve the activity and selectivity. In this respect, Su *et al.* successfully prepared a porous carbon loaded N,P bicoordination Mn single-atomic catalyst by phosphating a zeolite imidazole skeleton and subsequent pyrolysis. The Mn_1–N/P–C catalysts with an Mn–N_2–P atomic structure showed better catalytic activity than the related catalysts with an Mn–

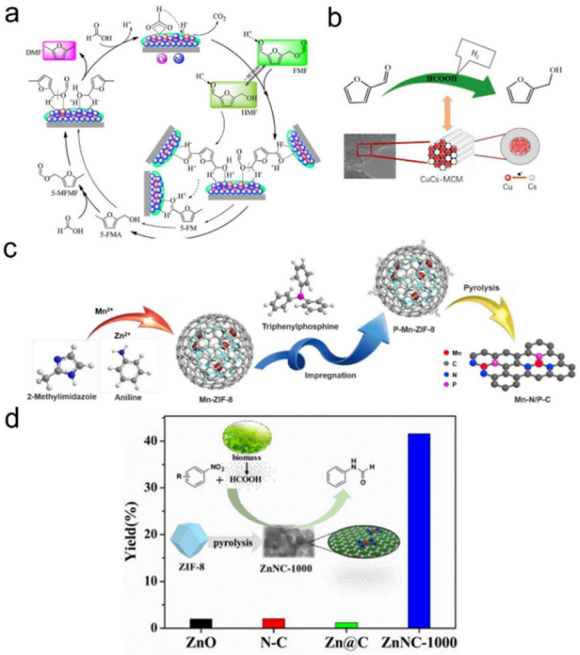

Fig. 7 (a) Schematic illustration for the conversion of FMF to DMF over the Ni–Cu bimetallic catalyst. Reproduced with permission from ref. 166. Copyright 2019 American Chemical Society. (b) Catalytic transfer hydrogenation of furfural to furfuryl alcohol over the CuCs-MCM catalyst. Reproduced with permission from ref. 167. Copyright 2021 Elsevier. (c) Schematic illustration of the synthetic process for Mn–N/P–C. Reproduced and modified with permission from ref. 168. Copyright 2022 American Chemical Society. (d) Atomically dispersed Zn–N_x sites in N-doped carbon for reductive *N*-formylation of nitroarenes. Reproduced with permission from ref. 169. Copyright 2019 Wiley-VCH.

N_x structure for the transfer hydrogenation of nitroaromatics with formic acid as the donor. It was found that doping of the P source played an important role in affecting the morphology and electronic properties of the catalyst, thus improving the performance of the catalyst. This was the first example of a Mn heterogeneous catalyst for nitroaromatic reduction, and also revealed that the Mn–N_2–P structure was a more promising alternative in heterogeneous catalysis (Fig. 7c).[168] Li *et al.* prepared a highly active, inexpensive and stable single-atomic Zn/N-doped porous carbon catalyst using a zeolite imidazoline skeleton precursor. The optimized ZnNC-1000 had a higher Zn content (5.2 wt%) and higher nitrogen content (6.73 wt%), thus showing promising catalytic performance in *N*-formylation of nitroaromatics in one pot with formic acid as the hydrogen donor and formylation agent. H_2–D_2 exchange reactions and HCOOH chemisorption experiments showed that atomically dispersed Zn–N_x species were essential for the activation of hydrogen and HCOOH molecules, which ultimately resulted in the highest catalytic activity for reducing carbamylation (Fig. 7d).[169]

2.2. Photocatalytic hydrogenation catalysts

Efficient and cost-effective usage of solar energy represents an extremely promising technology to solve global issues of energy and environment, thus realizing carbon neutrality.[170–176] Among them, photocatalytic hydrogenation has been regarded as an important strategy to convert solar energy into hydrogen energy and some key chemicals, involving three primary steps: light absorption, charge separation and transfer and subsequent catalytic hydrogenation.[22,23,177–180] However, the current systems still suffer from low conversion efficiency. The key scientific problem lies in how to design and develop highly efficient photocatalysts to improve the efficiency of each step and the whole process.

Lu *et al.* used SAPO-31 supported Pd single atoms and ultra-small cluster catalyst (Pd_{SA+C}/SAPO-31) to achieve hydrodeoxygenation of vanillin through a simple photochemical pathway. Under mild conditions (1 atm, 80 °C, 30 min), the selectivity of 2-methoxy-4-methylphenol and TOF were >99% and 3000 h^{-1} using formic acid as a hydrogen source, respectively. The high activity of the catalyst was due to the synergistic catalysis between the positively charged Pd single atoms and the fully exposed clusters and the strong metal–support interactions (Fig. 8a).[181] Tsutsumi *et al.* prepared a transition metal-supported silicon NP catalyst that achieved a photoinduced reduction of nitrobenzene to aniline using formic acid as a hydrogen source. By comparing M/Si (M = Pt, Ru, and Pd), Pd/Si was the most suitable catalyst for the photocatalytic conversion of nitrobenzene to aniline. They revealed that formic acid acted both as a hydrogen source and as a sacrificial reagent to introduce electrons into the semiconductor to form holes, and avoided the use of high-pressure equipment (Fig. 8b).[182] Considering that MOFs usually have high surface areas, high porosities and discrete active sites, they can therefore achieve efficient light absorption and charge transport by various modifications. Dong *et al.* prepared the Pd/MIL-101(Fe)-NH_2 catalyst with highly dispersed and uniform Pd NPs (~1.8 nm) by an *in situ* photodeposition

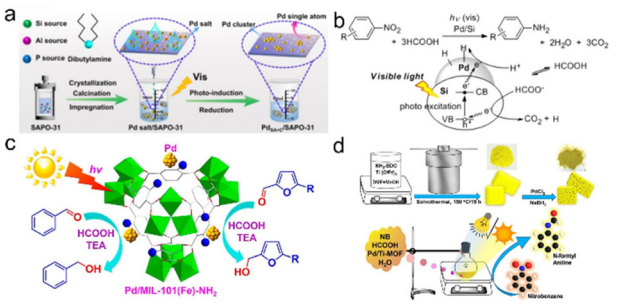

Fig. 8 (a) Schematic illustration for the construction and characterization of PdSA + C/SAPO-31. Reproduced and modified with permission from ref. 181. Copyright 2021 Springer Nature. (c) Photoinduced reduction of nitroarenes using a transition-metal-loaded silicon semiconductor. Reproduced with permission from ref. 182. Copyright 2016 American Chemical Society. (b) Photoinduced transfer hydrogenation of aromatic aldehydes by using Pd/MIL-101(Fe)-NH_2. Reproduced with permission from ref. 183. Copyright 2018 American Chemical Society. (d) Schematic Illustration of the synthesis of the Pd/Ti-MOF and the reaction setup used for the reductive *N*-formylation of NB. Reproduced with permission from ref. 184. Copyright 2022 American Chemical Society.

method. The dual role of the amine group on the support was embodied in stabilizing Pd NPs and enhancing the electron density in the Pd center. Under the conditions of triethylamine as the electron donor and HCOOH as the proton source, visible light induced selective transfer hydrogenation of aromatic aldehydes to produce corresponding alcohols was successfully realized (Fig. 8c).[183] Kar *et al.* prepared a visible-light photosensitive catalyst (Pd/Ti-MOF) by embedding Pd NPs in a titanium MOF, which can be used for photocatalytic reductive *N*-formylation of nitroarenes in water. The high photocatalytic performance of Pd/Ti-MOF can be attributed to the direct contact between Pd NPs and MOF, resulting in an abundance of catalytically active sites as well as superior electrical conductivity for a fast electron transfer process (Fig. 8d).[184]

3. Transfer hydrogenation using methanol as a hydrogen source

3.1. Catalyst design for thermocatalytic hydrogenation

In addition to formic acid, methanol produced from CO_2 direct reduction and petroleum and biomass chemical industry is also considered as a good hydrogen donor since it is inexpensive and easy to handle, involving environmentally benign by-products, do not require elaborate experimental setups, such as high pressure reactors, and are more stable than molecular hydrogen.[23,103,185] Compared with formic acid, methanol is less corrosive to experimental equipment and catalysts.

3.1.1 Precious metal-based heterogeneous catalysts. Like the formic acid system, the Pd site is one of the most effective and widely studied catalytically active sites due to its special electronic structure. Goyal *et al.* employed a commercial carbon-supported palladium (Pd/C) catalyst that catalyzed *N*-methylation of nitroaromatics and amines using methanol as the C1 and H source. More than thirty structurally diverse *N*-methylamine including bioactive compounds, were synthesized with a high yield of up to 95%. In addition, selective *N*-methylation and deuteration of the nonsteroidal anti-inflammatory drug nimesulide were achieved by late functionalization.[186] Lee *et al.* synthesized biodiesel from soybean oil by transesterification and catalytic transfer hydrogenation on Pd/ZSM-5 or commercial Pd/Al_2O_3 in methanol. Although the dispersion of Pd NPs on Pd/ZSM-5 was higher than that of Pd/Al_2O_3, the activity of Pd/ZSM-5 was lower due to the unique pore structure of ZSM-5.[187] In addition to the Pd site, Zhu *et al.* prepared a recyclable ZnO supported Ir catalyst for the transfer hydrogenation of aldehydes and ketones at 110 °C with methanol as the hydrogen source, and the yield of alcohol could reach 98%. The mechanism study showed that methanol was first dehydrogenated to formaldehyde, and then completely decomposed into active hydrogen species for subsequent hydrogenation. This excellent performance was related to the ratio of high positive charge IrO_x and its ultrahigh dispersion on ZnO. The fine coordination of IrO_x and ZnO enhanced the cleavage of O–H bonds and low-activity C–H bonds in methanol to form active hydrogen, so that methanol decomposition and C=O hydrogenation maintained a good balance in the transfer hydrogenation reaction.[188]

3.1.2. Nonprecious metal-based heterogeneous catalysts

Copper-based NP catalysts. Due to the superior activity of copper in hydrogen production from methanol, copper based catalysts have received the most attention in methanol promoted transfer hydrogenation. Yfanti *et al.* investigated the role of different hydrogen donors in the liquid-phase hydrogenation of glycerol to deoxypropylene glycol over the Cu : Zn : Al catalyst. They found that methanol was the best H donor (74% yield), followed by 2-propyl alcohol (59.6% yield) in terms of hydrogen production and 1,2-propylene glycol production. Formic acid was also a potential H donor, since its activity in catalyzing hydrogen transfer was more favorable at low H_2 donor/glycerol molar ratios (Fig. 9a).[189] Tang *et al.* performed the hydrocyclization of methyl levulinate in methanol on a nano-Cu catalyst without external H_2. The nanocrystalline Cu catalyst can be used as a bifunctional catalyst for hydrogen production by methanol reforming and methyl levulinate hydrogenation.[190] Zhang *et al.* synthesized a series of Cu-based catalysts with different supports (Cu/Al_2O_3, Cu/ZnO, Cu/ZrO_2 and Cu/CeO_2) to study the *in situ* hydrogenation of 5-hydroxymethylfurfural to 2,5-dimethylfuran using methanol as an economic hydrogen supplier. The results showed that different supports exhibited significant effects on the activity of methanol dehydrogenation and 5-hydroxymethylfurfural hydrogenation of Cu-based catalysts. The best catalytic activity of Cu/Al_2O_3 with the smallest grain size of Cu and the strongest acidity was attributed to the highest *in situ* hydrogen production activity of methanol.[191] Awan *et al.* tested a copper–nickel mixed catalyst prepared by calcination of iron and aluminium hydrotalcites (layered double hydroxides, LDH) in the conversion of a lignin model dimer in subcritical methanol. The presence of copper was essential for efficient hydrogenation, either through the direct transfer of hydrogen from methanol to aldehyde groups or through reactivity of methanol reforming products. TPR experiments showed that the enhanced reducibility of Cu catalysts promoted the hydrogenation activity, which was related to the presence of other oxide components. They showed that copper was formed by the reduction of CuO by methanol, and the modification of the oxide catalyst in the reaction medium played a major role in the formation of the active site.[192] Zhang *et al.* synthesized a ZrO_2-supported nano-Cu catalyst (monooblique ZrO_2: m-ZrO_2; tetragonal ZrO_2: t-ZrO_2). In the methanol–water system, the catalytic performance of the Cu/t-ZrO_2 catalyst for lauric acid hydrogenation was significantly better than that of the Cu/m-ZrO_2 catalyst. The low efficiency of m-ZrO_2 as a support was attributed to the weak adsorption of reactants and intermediate molecules and the absence of oxygen vacancy in the crystal phase. The DFT calculations further indicated that the metal–support interface played an important role in promoting the cleavage of C–O or H–H bonds in both possible reaction paths, thereby reducing the activation barrier of the whole reaction (Fig. 9b).[26] Zhang *et al.* screened a series of cheap Cu-based catalysts from hydrotalcite precursors using methanol as the

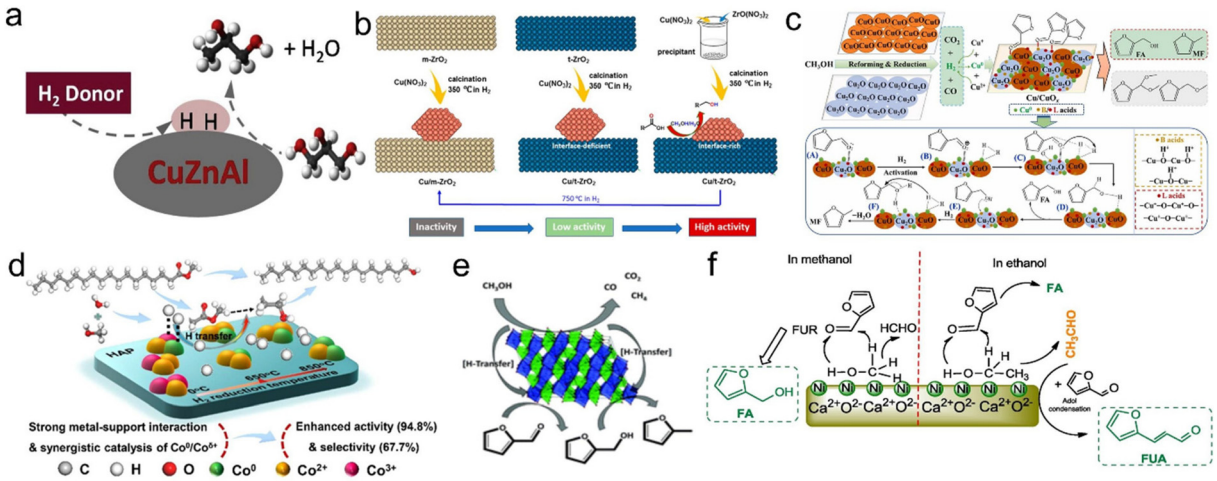

Fig. 9 (a) Hydrodeoxygenation of glycerol to 1,2-propanediol over the Cu : Zn : Al catalyst. Reproduced and modified with permission from ref. 189. Copyright 2020 Elsevier. (b) Schematic diagram of the synthesis of Cu/ZrO_2 *via* different preparation methods and reduction temperatures. Reproduced with permission from ref. 26. Copyright 2020 American Chemical Society. (c) The catalytic mechanism for methanol-mediated H-transfer transformation of furfural over CuO_x. Reproduced with permission from ref. 194. Copyright 2022 Elsevier. (d) Schematic illustration of the catalytic transfer hydrogenation over synergistic Co/HAP catalysts. Reproduced with permission from ref. 196. Copyright 2021 American Chemical Society. (e) The gas-phase production of 2-methylfurfural using a $FeVO_4$ catalyst. Reproduced with permission from ref. 197. Copyright 2017 Royal Society of Chemistry. (f) The catalytic reaction mechanism for conversion of FUR in aliphatic alcohol. Reproduced with permission from ref. 198. Copyright 2019 Elsevier.

solvent and hydrogen donor to selectively transfer hydrogenate furfural to furfuryl alcohol and 2-methylfuran. The Cu-based catalyst had good selectivity for transfer hydrogenation of furfural to furfuryl alcohol, and the furfuryl alcohol yield in 473 K methanol was 94.0 mol%. The Cu catalyst used CuO and Cu_2O as catalysts and methanol as a hydrogen source to conduct transfer hydrogenation of furfural. The characterization and experimental results showed that the conversion of furfural–furfuryl alcohol and furfural-2-methylfuran depended largely on the hydrogen production, and furfural-2-methylfuran was further treated with H_2/N_2 at 773 K and Cu was formed in the activated sample. Interestingly, the resulting activated copper catalyst was favorable for the conversion of furfural to 2-methylfuran with a yield of 94.1 mol% at 513 K.[193] Zhang *et al.* determined the capacity of methanol reforming and the adsorption strength of furfural on CuO_x. DFT calculations showed that the CuO (200) surface had low free energy and energy barrier for methanol reforming and furfural transfer hydrogenation (Fig. 9c).[194] Besides, Li *et al.* prepared the $Cu^0/Cu_2O{\cdot}SiO_2$ catalyst, which can selectively generate 2-methylfuran with a yield of 90% from furfural at 220 °C within 2 h. Methanol was used *in situ* to produce high purity hydrogen (92% content), and the nearly CO free atmosphere avoided toxicity at Cu sites. The structure–activity relationship showed that Cu^0 or Cu_2O or the physical mixture of Cu^0 and Cu_2O had no activity, but the hydrogen-reduced layered copper silicate samples with a rich $Cu^0/Cu_2O{\cdot}SiO_2$ interface had high activity in both methanol decomposition and furfural hydrodeoxygenation reactions.[195]

In addition to the copper site, Yao *et al.* studied the catalytic transfer hydrogenation of methyl stearate to octadecyl alcohol with methanol and water as hydrogen donors over the Co/hydroxyapatite catalyst. Characterization and DFT calculations showed that the strong interaction between Co and hydroxyapatite support in the catalyst enhanced the electron transfer ability, and the combination of $Co^0/Co^{\delta+}$ active sites can synergically promote H_2 formation and hydrogenation of methyl stearate in the methanol/water system (Fig. 9d).[196] Grazia *et al.* studied the process of producing 2-methylfuran in the gas phase of furfural using methanol as H transfer agent and $FeVO_4$ as the catalyst. At 320 °C, the yield of 2-methylfuran can reach 80%, with small amounts of 2,5-dimethylfuran and 2-vinylfuran as byproducts. The characterization of the catalyst indicated that the reduction of $FeVO_4$ occurred under real conditions, leading to the *in situ* development of the truly active phase (Fig. 9e).[197] Zhang *et al.* prepared a novel Ni@R–Ca catalyst for catalytic transfer hydrogenation of furfural under mild reaction conditions. With methanol as the reaction medium, furfuryl alcohol can be obtained as the only product with a 99% yield. The synergistic effect of metal Ni and R–Ca lattice played a crucial role in the efficient transformation of furfural (Fig. 9f).[198] Luo *et al.* investigated the synergistic effect of Fe and Ni over Ni–Fe/SBA-15 catalysts for the synthesis of γ-valerolactone from levulinic acid with methanol as the only hydrogen donor. The results of H_2-TPD and XPS indicated that electron transfer occurred from Fe to Ni, which was favorable for the activation of the C=O bond and dissociative activation of the H_2 molecule.[199]

3.2 Photocatalytic hydrogenation catalysts

First, pure semiconductors such as TiO_2 show excellent conversions and selectivities for this photocatalytic hydrogenation.

Wu *et al.* found that selective conversion of the key lignocellulosic platform compounds such as furfural and vanillin could be achieved through photocatalysis by controlling the TiO_2 exposure surface. The surface dependent density of oxygen vacancy determined the charge distribution and adsorption strength of surface species, thus controlling the selectivity of products (Fig. 10a).[200] Besides, Zhao *et al.* designed a photocatalytic transfer hydrogenation system using solar energy as energy input and methanol as the hydrogen source. In this respect, the Pd–Pt/TiO_2 bimetallic alloy catalyst showed significantly better photocatalytic performance than Pd/TiO_2 or Pt/TiO_2 alone. They revealed holes with strong oxidation ability spread to the surface of TiO_2, triggering the oxidation of adsorbed methanol into formaldehyde or other deep oxidation products, accompanied by the release of hydrogen ions. Photoinduced electrons on the surface of the precious metal reduced protons to hydrogen atoms, thus forming surface hydrides that can react with the unsaturated C=O or C=C groups of the substrate molecules adsorbed on the surface (Fig. 10b).[201] Jian *et al.* developed a new strategy to control the activity/selectivity of biomass reduction upgrading to biofuels at room temperature by engineering oxygen vacancies and manipulating the exposed crystal surfaces of TiO_2-based catalysts. The (101) crystal plane was more likely to generate more oxygen vacancies *in situ* than the (001) and (110) crystal planes. And the formation of oxygen vacancies was not only beneficial for the adsorption and activation of biobased carbonyl, but also can improve the migration efficiency of photogenerated carrier, effectively adjusting the semiconductor band structure of the TiO_2-based photocatalyst and promoting visible light absorption, and thus improve the overall reduction and transformation process (Fig. 10c).[202]

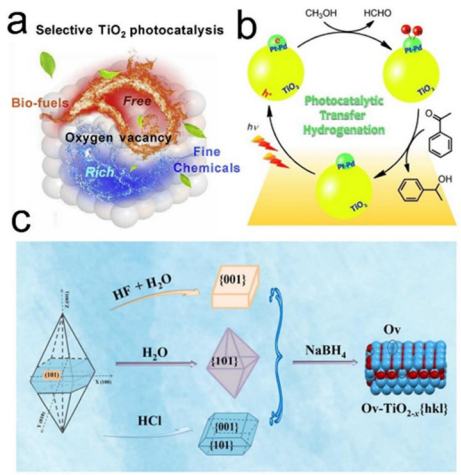

Fig. 10 (a) Schematic illustration for the selectivity control by surface engineering of titanium oxide. Reproduced with permission from ref. 200. Copyright 2020 Elsevier. (b) The catalytic reaction mechanism for transfer hydrogenation on the Pd–Pt alloy cocatalyst. Reproduced with permission from ref. 201. Copyright 2014 Wiley-VCH. (c) Preparation schematic of TiO_2-based catalysts with different crystal surfaces and specific oxygen vacancy (Ov). Reproduced with permission from ref. 202. Copyright 2022 Elsevier.

4. Conclusion

In this review, we have presented the recent progress in the development of heterogeneous catalysts with excellent catalytic performance for transfer hydrogenation reactions using formic acid and methanol as the hydrogen sources by thermocatalytic

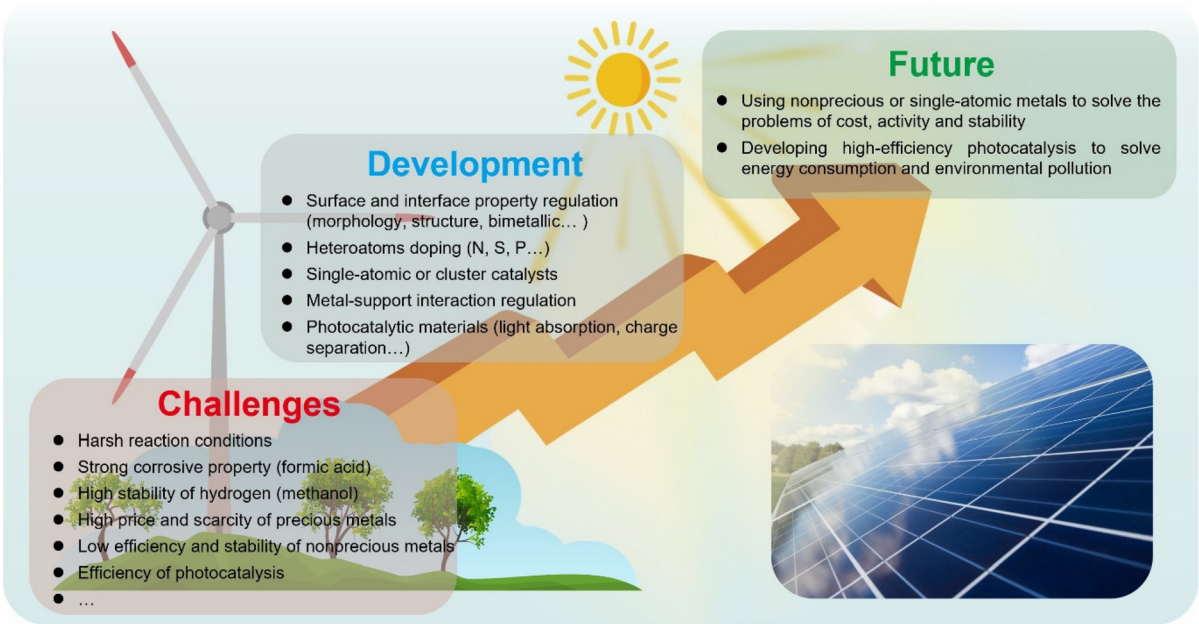

Scheme 4 The proposed challenges and opportunities for the development of heterogeneous catalysts in this area.

and photocatalytic strategies. Many efforts have been made to realize the rational design and synthesis of highly efficient catalysts. However, there are some challenges and opportunities for future work in this area as follows (Scheme 4):

For transfer hydrogenation using formic acid as the hydrogen source, the catalyst stability remains the biggest challenge due to the corrosive nature of formic acid solutions, especially for the nonprecious ones. In order to reduce coke deposition and metal leaching, strengthening the interactions between metals and supports or adding some protective layers such as carbon layers will be effective, but it will inevitably affect the catalytic activity. Therefore, it is a key scientific issue to develop new synthetic routes to achieve simultaneous improvement of activity and stability. Given the cost and scarcity, a nonprecious metal catalyst is a better choice, and a single-atom catalyst may be a big breakthrough. Photocatalysis or electrocatalysis technology also needs to be introduced into the system to solve the problem of excessive energy consumption and environmental pollution, but it needs separation and purification technologies.

For transfer hydrogenation using methanol as the hydrogen source, the decomposition of methanol to produce hydrogen is a difficult issue. The methanol systems usually require harsh reaction conditions such as high reaction temperature, which require the design and synthesis of efficient catalysts to make the reaction conditions milder. Recently, photocatalytic hydrogen generation of methanol has been developed rapidly, which means that photocatalytic technology may be a way to achieve this kind of transfer hydrogenation. The catalyst stability is also an important issue for practical applications, and it is a feasible strategy to develop catalysts with a special structure which is conducive to strengthening metal–support interactions.

Finally, we hope that our review will provide a clearer picture for researchers in related fields, as well as serve as a guide for future research direction.

Author contributions

YX, RL and WG conceptualized and designed the review's theme and framework. GC, JM, JL and ZL conducted data collection and literature analysis. GC, JM and WG wrote the original draft. All authors reviewed and edited the draft.

Conflicts of interest

There are no conflicts to declare.

Acknowledgements

This work was supported by the National Key R&D Program of China (2020YFA0406103), NSFC (21725102, 51902311, 22122506, 91961106, 22075267, 22232003, and 22109148), the Strategic Priority Research Program of the CAS (XDPB14), the Anhui Provincial Natural Science Foundation (2008085J05), the Youth Innovation Promotion Association of CAS (2019444), the Users with Excellence Program of Hefei Science Center CAS (2020HSC-UE003) and the Fundamental Research Funds for the Central Universities (WK2060000039 and 20720220007).

References

1 S. Pang, S. Jin, F. Yang, M. Alberts, L. Li, D. Xi, R. G. Gordon, P. Wang, M. J. Aziz and Y. Ji, *Nat. Energy*, 2023, **8**, 1126–1136.
2 H. Seo and T. A. Hatton, *Nat. Commun.*, 2023, **14**, 313.
3 Y. S. Xia, M. Z. Tang, L. Zhang, J. Liu, C. Jiang, G. K. Gao, L. Z. Dong, L. G. Xie and Y. Q. Lan, *Nat. Commun.*, 2022, **13**, 2964.
4 S. Fang, M. Rahaman, J. Bharti, E. Reisner, M. Robert, G. A. Ozin and Y. H. Hu, *Nat. Rev. Methods Primers*, 2023, **3**, 61.
5 C. J. Hu, Z. W. Jiang, Q. Y. Wu, S. Y. Cao, Q. H. Li, C. Chen, L. Y. Yuan, Y. L. Wang, W. Y. Yang, J. B. Yang, J. Peng, W. Q. Shi, M. L. Zhai, M. Mostafavi and J. Ma, *Nat. Commun.*, 2023, **14**, 4767.
6 P. De Luna, C. Hahn, D. Higgins, S. A. Jaffer, T. F. Jaramillo and E. H. Sargent, *Science*, 2019, **364**, eaav3506.
7 H. Chen, H. Dong, Z. Y. Shi and A. K. SenGupta, *Sci. Adv.*, 2023, **9**, eadg1956.
8 J. X. Zhu, J. T. Li, R. H. Lu, R. H. Yu, S. Y. Zhao, C. B. Li, L. Lv, L. X. Xia, X. B. Chen, W. W. Cai, J. S. Meng, W. Zhang, X. L. Pan, X. F. Hong, Y. H. Dai, Y. Mao, J. Li, L. Zhou, G. J. He, Q. Q. Pang, Y. Zhao, C. Xia, Z. Y. Wang, L. M. Dai and L. Q. Mai, *Nat. Commun.*, 2023, **14**, 4670.
9 S. Yang, H. Y. An, S. Arnouts, H. Wang, X. Yu, J. de Ruiter, S. Bals, T. Altantzis, B. M. Weckhuysen and W. van der Stam, *Nat. Catal.*, 2023, **6**, 796–806.
10 T. Sengupta and S. N. Khanna, *Commun. Chem.*, 2023, **6**, 53.
11 J. J. Su, C. B. Musgrave, Y. Song, L. B. Huang, Y. Liu, G. Li, Y. E. Xin, P. Xiong, M. M. J. Li, H. R. Wu, M. H. Zhu, H. M. Chen, J. Y. Zhang, H. C. Shen, B. Z. Tang, M. Robert, W. I. I. I. Goddard and R. Q. Ye, *Nat. Catal.*, 2023, **6**, 818–828.
12 H. Zhou, Z. X. Chen, A. V. López, E. D. López, E. Lam, A. Tsoukalou, E. Willinger, D. A. Kuznetsov, D. Mance, A. Kierzkowska, F. Donat, P. M. Abdala, A. Comas-Vives, C. Copéret, A. Fedorov and C. R. Müller, *Nat. Catal.*, 2021, **4**, 860–871.
13 A. Álvarez, A. Bansode, A. Urakawa, A. V. Bavykina, T. A. Wezendonk, M. Makkee, J. Gascon and F. Kapteijn, *Chem. Rev.*, 2017, **117**, 9804–9838.
14 J. Lim, A. T. Garcia-Esparza, J. W. Lee, G. Kang, S. Shin, S. S. Jeon and H. Lee, *Nanoscale*, 2022, **14**, 9297–9303.
15 M. Farajzadeh, H. Alamgholiloo, F. Nasibipour, R. Banaei and S. Rostamnia, *Sci. Rep.*, 2020, **10**, 18188.

16 C. J. Zhan, X. W. Li, G. X. Lan, E. E. K. Baidoo, Y. K. Yang, Y. Z. Liu, Y. Sun, S. J. Wang, Y. Y. Wang, G. K. Wang, J. Nielsen, J. D. Keasling, Y. Chen and Z. H. Bai, *Nat. Catal.*, 2023, **6**, 435–450.
17 M. Y. He, Y. H. Sun and B. X. Han, *Angew. Chem., Int. Ed.*, 2022, **61**, e202112835.
18 P. Hauke, T. Merzdorf, M. Klingenhof and P. Strasser, *Nat. Commun.*, 2023, **14**, 4708.
19 A. Parastaev, V. Muravev, E. H. Osta, T. F. Kimpel, J. F. M. Simons, A. J. F. van Hoof, E. Uslamin, L. Zhang, J. J. C. Struijs, D. B. Burueva, E. V. Pokochueva, K. V. Kovtunov, I. V. Koptyug, I. J. Villar-Garcia, C. Escudero, T. Altantzis, P. Liu, A. Béché, S. Bals, N. Kosinov and E. J. M. Hensen, *Nat. Catal.*, 2022, **5**, 1051–1060.
20 G. Han, G. Li and Y. Sun, *Nat. Catal.*, 2023, **6**, 224–233.
21 D. D. Mu, Z. W. Li, S. Y. Yu and S. T. Liu, *Catal. Today*, 2022, **402**, 67–78.
22 M. Guo, M. Zhang, R. Liu, X. Zhang and G. Li, *Adv. Sci.*, 2021, **9**, 2103361.
23 J. J. Song, Z. F. Huang, L. Pan, K. Li, X. W. Zhang, L. Wang and J. J. Zou, *Appl. Catal., B*, 2018, **227**, 386–408.
24 J. J. Wu, Z. Y. Chen, J. H. Barnard, R. Gunasekar, C. Y. Pu, X. F. Wu, S. Y. Zhang, J. W. Ruan and J. L. Xiao, *Nat. Catal.*, 2022, **5**, 982–992.
25 H. Y. Xu, P. Yang, P. Chuanprasit, H. Hirao and J. R. Zhou, *Angew. Chem., Int. Ed.*, 2015, **54**, 5112–5116.
26 Z. H. Zhang, M. Z. Jing, H. Chen, F. Okejiri, J. X. Liu, Y. Leng, H. L. Liu, W. Y. Song, Z. Y. Hou, X. Y. Lu, J. Fu and J. Liu, *ACS Catal.*, 2020, **10**, 9098–9108.
27 A. Kumar, P. Daw and D. Milstein, *Chem. Rev.*, 2022, **122**, 385–441.
28 F. J. Zhao, T. X. Xu, G. M. Zhu, K. Wang, X. Xu and L. Liu, *Sustainable Energy Fuels*, 2022, **6**, 1866–1890.
29 Z. D. An and J. Li, *Green Chem.*, 2022, **24**, 1780–1808.
30 T. K. Das, A. M. R. Treviño, S. Pandiri, S. Irvankoski, J. H. Siitonen, S. M. Rodriguez, M. Yousufuddin and L. Kürti, *Green Chem.*, 2023, **25**, 746–754.
31 K. Azouzi, D. A. Valyaev, S. Bastin and J. B. Sortais, *Curr. Opin. Green Sustainable Chem.*, 2021, **31**, 100511.
32 S. Mudhulu, Z. J. Gong, H. C. Ku, Y. H. Lu and W. Y. Yu, *Mater. Today Sustain.*, 2022, **19**, 100199.
33 A. Modak, D. Gill, A. R. Mankar, K. K. Pant, V. Bhasin, C. Nayak and S. Bhattacharya, *Nanoscale*, 2022, **14**, 15875–15888.
34 M. J. Gilkey and B. J. Xu, *ACS Catal.*, 2016, **6**, 1420–1436.
35 M. Niermann, S. Drünert, M. Kaltschmitt and K. Bonhoff, *Energy Environ. Sci.*, 2019, **12**, 290–307.
36 J. Eppinger and K. W. Huang, *ACS Energy Lett.*, 2017, **2**, 188–195.
37 R. van Putten, T. Wissink, T. Swinkels and E. A. Pidko, *Int. J. Hydrogen Energy*, 2019, **44**, 28533–28541.
38 S. Kar, M. Rauch, G. Leitus, Y. Ben-David and D. Milstein, *Nat. Catal.*, 2021, **4**, 193–201.
39 D. Wei, R. Sang, P. Sponholz, H. Junge and M. Beller, *Nat. Energy*, 2022, **7**, 438–447.
40 A. Mahmood, W. H. Guo, H. Tabassum and R. Q. Zou, *Adv. Energy Mater.*, 2016, **6**, 1600423.
41 S. Zhai, S. Jiang, C. Liu, Z. Li, T. Yu, L. Sun, G. Ren and W. Deng, *J. Phys. Chem. Lett.*, 2022, **13**, 8586–8600.
42 S. Keshipour and S. Mohammad-Alizadeh, *Sci. Rep.*, 2021, **11**, 16148.
43 A. Boddien, D. Mellmann, F. Gärtner, R. Jackstell, H. Junge, P. J. Dyson, G. Laurenczy, R. Ludwig and M. Beller, *Science*, 2011, **333**, 1733–1736.
44 J. J. A. Celaje, Z. Y. Lu, E. A. Kedzie, N. J. Terrile, J. N. Lo and T. J. Williams, *Nat. Commun.*, 2016, **7**, 11308.
45 Z. H. Yu, X. B. Lu, L. H. Sun, J. Xiong, L. Ye, X. Y. Li, R. Zhang and N. Ji, *ACS Sustainable Chem. Eng.*, 2021, **9**, 2990–3010.
46 X. Li, A. E. Surkus, J. Rabeah, M. Anwar, S. Dastigir, H. Junge, A. Brückner and M. Beller, *Angew. Chem., Int. Ed.*, 2020, **59**, 15849–15854.
47 R. Xu, W. Q. Lu, S. Toan, Z. R. Zhou, C. K. Russell, Z. Sun and Z. Q. Sun, *J. Mater. Chem. A*, 2021, **9**, 24241–24260.
48 S. J. Li, Y. T. Zhou, X. Kang, D. X. Liu, L. Gu, Q. H. Zhang, J. M. Yan and Q. Jiang, *Adv. Mater.*, 2019, **31**, 1806781.
49 S. A. Burgess, A. Kassie, S. A. Baranowski, K. J. Fritzsching, K. Schmidt-Rohr, C. M. Brown and C. R. Wade, *J. Am. Chem. Soc.*, 2016, **138**, 1780–1783.
50 J. M. Zimbron, M. Dauphinais and A. B. Charette, *Green Chem.*, 2015, **17**, 3255–3259.
51 L. Liu, H. Gao, S. Q. Yang, X. C. Chen, Y. Lu, Y. Liu and F. Xia, *J. Catal.*, 2020, **385**, 183–193.
52 K. Lu, X. Kong, J. M. Cai, S. R. Yu and X. G. Zhang, *Nanoscale*, 2023, **15**, 8084–8109.
53 C. Yu, X. F. Guo, B. Shen, Z. Xi, Q. Li, Z. Y. Yin, H. Liu, M. Muzzio, M. Q. Shen, J. R. Li, C. T. Seto and S. H. Sun, *J. Mater. Chem. A*, 2018, **6**, 23766–23772.
54 X. L. Cui, Y. Long, X. Zhou, G. Q. Yu, J. Yang, M. Yuan, J. T. Ma and Z. P. Dong, *Green Chem.*, 2018, **20**, 1121–1130.
55 M. López Granados, J. Moreno, A. C. Alba-Rubio, J. Iglesias, D. Martín Alonso and R. Mariscal, *Green Chem.*, 2020, **22**, 1859–1872.
56 R. F. Nie, Y. W. Tao, Y. Q. Nie, T. L. Lu, J. S. Wang, Y. S. Zhang, X. Y. Lu and C. C. Xu, *ACS Catal.*, 2021, **11**, 1071–1095.
57 R. V. Jagadeesh, D. Banerjee, P. B. Arockiam, H. Junge, K. Junge, M. M. Pohl, J. Radnik, A. Brückner and M. Beller, *Green Chem.*, 2015, **17**, 898–902.
58 Y. N. Duan, T. Song, X. S. Dong and Y. Yang, *Green Chem.*, 2018, **20**, 2821–2828.
59 Y. H. Han, Z. Y. Wang, R. R. Xu, W. Zhang, W. X. Chen, L. R. Zheng, J. Zhang, J. Luo, K. L. Wu, Y. Q. Zhu, C. Chen, Q. Peng, Q. Liu, P. Hu, D. S. Wang and Y. D. Li, *Angew. Chem., Int. Ed.*, 2018, **57**, 11262–11266.
60 F. Chen, B. Sahoo, C. Kreyenschulte, H. Lund, M. Zeng, L. He, K. Junge and M. Beller, *Chem. Sci.*, 2017, **8**, 6239–6246.
61 M. Yuan, Y. Long, J. Yang, X. W. Hu, D. Xu, Y. Y. Zhu and Z. P. Dong, *ChemSusChem*, 2018, **11**, 4156–4165.

62 A. K. Kar and R. Srivastava, *ACS Sustainable Chem. Eng.*, 2019, **7**, 13136–13147.
63 I. Sorribes, K. Junge and M. Beller, *Chem. – Eur. J.*, 2014, **20**, 7878–7883.
64 Y. T. Chen, *Chem. – Eur. J.*, 2019, **25**, 3405–3439.
65 S. Savourey, G. Lefèvre, J. C. Berthet and T. Cantat, *Chem. Commun.*, 2014, **50**, 14033–14036.
66 X. Jiang, C. Wang, Y. W. Wei, D. Xue, Z. T. Liu and J. L. Xiao, *Chem. – Eur. J.*, 2014, **20**, 58–63.
67 V. Yadav, G. Sivakumar, V. Gupta and E. Balaraman, *ACS Catal.*, 2021, **11**, 14712–14726.
68 U. Eberle, M. Felderhoff and F. Schüth, *Angew. Chem., Int. Ed.*, 2009, **48**, 6608–6630.
69 L. L. Lin, W. Zhou, R. Gao, S. Y. Yao, X. Zhang, W. Q. Xu, S. J. Zheng, Z. Jiang, Q. L. Yu, Y. W. Li, C. Shi, X. D. Wen and D. Ma, *Nature*, 2017, **544**, 80–83.
70 J. Zheng, H. Zhou, C. G. Wang, E. Y. Ye, J. W. Xu, X. J. Loh and Z. B. Li, *Energy Storage Mater.*, 2021, **35**, 695–722.
71 F. Valentini, A. Marrocchi and L. Vaccaro, *Adv. Energy Mater.*, 2022, **12**, 2103362.
72 Y. Wang, J. F. Han, N. Wang, B. Li, M. Yang, Y. M. Wu, Z. X. Jiang, Y. X. Wei, P. Tian and Z. M. Liu, *Chin. J. Catal.*, 2022, **43**, 2259–2269.
73 J. B. Zhou, M. B. Gao, J. L. Zhang, W. J. Liu, T. Zhang, H. Li, Z. C. Xu, M. Ye and Z. M. Liu, *Nat. Commun.*, 2021, **12**, 17.
74 M. Yang, D. Fan, Y. X. Wei, P. Tian and Z. M. Liu, *Adv. Mater.*, 2019, **31**, 1902181.
75 E. Ebadzadeh, M. H. Khademi and M. Beheshti, *Chem. Eng. J.*, 2021, **405**, 126605.
76 A. Hwang and A. Bhan, *Acc. Chem. Res.*, 2019, **52**, 2647–2656.
77 I. Lezcano-Gonzalez, E. Campbell, A. E. J. Hoffman, M. Bocus, I. V. Sazanovich, M. Towrie, M. Agote-Aran, E. K. Gibson, A. Greenaway, K. De Wispelaere, V. Van Speybroeck and A. M. Beale, *Nat. Mater.*, 2020, **19**, 1081–1087.
78 X. J. Cui, R. Huang and D. H. Deng, *EnergyChem*, 2021, **3**, 100050.
79 Y. F. Ma, G. Q. Guan, C. Shi, A. M. Zhu, X. G. Hao, Z. D. Wang, K. Kusakabe and A. Abudula, *Int. J. Hydrogen Energy*, 2014, **39**, 258–266.
80 M. Nielsen, E. Alberico, W. Baumann, H. J. Drexler, H. Junge, S. Gladiali and M. Beller, *Nature*, 2013, **495**, 85–89.
81 L. López-Rodríguez, D. G. Araiza, D. G. Arcos, A. Gómez-Cortés and G. Díaz, *Catal. Today*, 2022, **394–396**, 486–498.
82 T. Tsoncheva, I. Genova, M. Stoyanova, M. M. Pohl, R. Nickolov, M. Dimitrov, E. Sarcadi-Priboczki, M. Mihaylov, D. Kovacheva and K. Hadjiivanov, *Appl. Catal., B*, 2014, **147**, 684–697.
83 N. Koivikko, T. Laitinen, S. Ojala, S. Pitkäaho, A. Kucherov and R. L. Keiski, *Appl. Catal., B*, 2011, **103**, 72–78.
84 G. C. Behera and K. Parida, *Chem. Eng. J.*, 2012, **180**, 270–276.
85 J. H. Kim, Y. S. Jang and D. H. Kim, *Chem. Eng. J.*, 2018, **338**, 752–763.
86 Q. Wang, J. L. Lan, R. Liang, Y. H. Xia, L. Qin, L. W. Chung and Z. P. Zheng, *ACS Catal.*, 2022, **12**, 2212–2222.
87 G. K. Hu, J. Y. Wang, X. Zhang, D. Liu, B. Yu, T. Huang, M. F. Zhu and H. Yu, *Carbon*, 2023, **214**, 118311.
88 D. R. Palo, R. A. Dagle and J. D. Holladay, *Chem. Rev.*, 2007, **107**, 3992–4021.
89 L. Li, L. Zhang, L. Gou, S. Wei, X. Hou and L. Wu, *Chem. Eng. J.*, 2023, **454**, 140292.
90 Y. Tong, X. Yan, J. Liang and S. X. Dou, *Small*, 2019, **17**, 1904126.
91 N. Z. Liu, R. X. Wang, S. J. Gao, R. F. Zhang, F. R. Fan, Y. H. Ma, X. L. Luo, D. Ding and W. Z. Wu, *Nano Energy*, 2023, **109**, 108311.
92 J. X. Liu, J. J. Hinsch, H. J. Yin, P. R. Liu, H. J. Zhao and Y. Wang, *J. Electroanal. Chem.*, 2022, **907**, 116071.
93 J. Chen, M. Ahmad, Y. Zhang, H. Ye, L. Wang, J. Zhang, X.-Z. Fu and J.-L. Luo, *Chem. Eng. J.*, 2023, **454**, 140056.
94 H. J. Yin, Y. H. Dou, S. Chen, Z. J. Zhu, P. R. Liu and H. J. Zhao, *Adv. Mater.*, 2020, **32**, 1904870.
95 Y. Guo, X. Yang, X. Liu, X. Tong and N. Yang, *Adv. Funct. Mater.*, 2022, **33**, 2209134.
96 Z. H. Li, X. Zhang, J. J. Liu, R. Shi, G. I. N. Waterhouse, X. D. Wen and T. R. Zhang, *Adv. Mater.*, 2021, **33**, 2103248.
97 Z. H. Li, J. J. Liu, Y. F. Zhao, R. Shi, G. I. N. Waterhouse, Y. S. Wang, L. Z. Wu, C. H. Tung and T. R. Zhang, *Nano Energy*, 2019, **60**, 467–475.
98 L. Y. Wu, Y. F. Mu, X. X. Guo, W. Zhang, Z. M. Zhang, M. Zhang and T. B. Lu, *Angew. Chem., Int. Ed.*, 2019, **58**, 9491–9495.
99 X. L. Zhao, S. Chen, H. J. Yin, S. Y. Jiang, K. Zhao, J. Kang, P. F. Liu, L. X. Jiang, Z. J. Zhu, D. D. Cui, P. R. Liu, X. J. Han, H. G. Yang and H. J. Zhao, *Matter*, 2020, **3**, 935–949.
100 Z. Li, J. Liu, J. Zhao, R. Shi, G. I. N. Waterhouse, X. D. Wen and T. Zhang, *Adv. Funct. Mater.*, 2022, **33**, 2213672.
101 Z. C. Zhang, X. C. Tian, B. W. Zhang, L. Huang, F. C. Zhu, X. M. Qu, L. Liu, S. Liu, Y. X. Jiang and S. G. Sun, *Nano Energy*, 2017, **34**, 224–232.
102 X. Xu, T. Lan, G. Zhao, Q. Nie, F. Jiang and Y. Lu, *Appl. Catal., B*, 2023, **334**, 122839.
103 H. Wang, H. F. Qi, X. Sun, S. Y. Jia, X. Y. Li, T. J. Miao, L. Q. Xiong, S. H. Wang, X. L. Zhang, X. Y. Liu, A. Q. Wang, T. Zhang, W. X. Huang and J. W. Tang, *Nat. Mater.*, 2023, **22**, 619–626.
104 L. Wang, Y. Sun, F. Zhang, J. Hu, W. Hu, S. Xie, Y. Wang, J. Feng, Y. Li, G. Wang, B. Zhang, H. Wang, Q. Zhang and Y. Wang, *Adv. Mater.*, 2022, **35**, 2205782.
105 X. X. Qin, H. Li, S. H. Xie, K. Li, T. W. Jiang, X. Y. Ma, K. Jiang, Q. Zhang, O. Terasaki, Z. J. Wu and W. B. Cai, *ACS Catal.*, 2020, **10**, 3921–3932.

106 O. Altan, E. Altintas, S. Alemdar and Ö. Metin, *Chem. Eng. J.*, 2022, **441**, 136047.
107 J. X. Fan, H. X. Du, Y. Zhao, Q. Wang, Y. N. Liu, D. Q. Li and J. T. Feng, *ACS Catal.*, 2020, **10**, 13560–13583.
108 D. I. Enache, J. K. Edwards, P. Landon, B. Solsona-Espriu, A. F. Carley, A. A. Herzing, M. Watanabe, C. J. Kiely, D. W. Knight and G. J. Hutchings, *Science*, 2006, **311**, 362–365.
109 M. Bonarowska, Z. Kaszkur, D. Lomot, M. Rawski and Z. Karpinski, *Appl. Catal., B*, 2015, **162**, 45–56.
110 L. Zhang, Z. X. Xie and J. L. Gong, *Chem. Soc. Rev.*, 2016, **45**, 3916–3934.
111 H. Doucet and J. C. Hierso, *Angew. Chem., Int. Ed.*, 2007, **46**, 834–871.
112 S. Mohanapriya and D. Gopi, *Renewable Sustainable Energy Rev.*, 2021, **148**, 111211.
113 T. W. van Deelen, C. Hernández Mejía and K. P. de Jong, *Nat. Catal.*, 2019, **2**, 955–970.
114 H. B. Zhang, G. G. Liu, L. Shi and J. H. Ye, *Adv. Energy Mater.*, 2018, **8**, 1701343.
115 X. B. Fan, G. L. Zhang and F. B. Zhang, *Chem. Soc. Rev.*, 2015, **44**, 3023–3035.
116 X. N. Li, X. F. Yang, Y. Q. Huang, T. Zhang and B. Liu, *Adv. Mater.*, 2019, **31**, 1902031.
117 A. T. Bell, *Science*, 2003, **299**, 1688–1691.
118 C. Y. Dong, Y. L. Li, D. Y. Cheng, M. T. Zhang, J. J. Liu, Y. G. Wang, D. Q. Xiao and D. Ma, *ACS Catal.*, 2020, **10**, 11011–11045.
119 R. Gusain, N. Kumar and S. S. Ray, *Coord. Chem. Rev.*, 2020, **405**, 213111.
120 Y. Wang, J. Chen, H. Ihara, M. Guan and H. D. Qiu, *TrAC, Trends Anal. Chem.*, 2021, **143**, 116421.
121 F. Marpaung, M. Kim, J. H. Khan, K. Konstantinov, Y. Yamauchi, M. S. A. Hossain, J. Na and J. Kim, *Chem. – Asian J.*, 2019, **14**, 1331–1343.
122 J. C. Ren, Y. L. Huang, H. Zhu, B. H. Zhang, H. K. Zhu, S. H. Shen, G. Q. Tan, F. Wu, H. He, S. Lan, X. H. Xia and Q. Liu, *Carbon Energy*, 2020, **2**, 176–202.
123 Y. P. Zhai, Y. Q. Dou, D. Y. Zhao, P. F. Fulvio, R. T. Mayes and S. Dai, *Adv. Mater.*, 2011, **23**, 4828–4850.
124 Q. Q. Yan, D. X. Wu, S. Q. Chu, Z. Q. Chen, Y. Lin, M. X. Chen, J. Zhang, X. J. Wu and H. W. Liang, *Nat. Commun.*, 2019, **10**, 4977.
125 L. He, F. Weniger, H. Neumann and M. Beller, *Angew. Chem., Int. Ed.*, 2016, **55**, 12582–12594.
126 W. Y. Ni, J. L. Meibom, N. Ul Hassan, M. Y. Chang, Y. C. Chu, A. Krammer, S. L. Sun, Y. W. Zheng, L. C. Bai, W. C. Ma, S. Lee, S. Jin, J. S. Luterbacher, A. Schüler, H. M. Chen, W. E. Mustain and X. L. Hu, *Nat. Catal.*, 2023, **6**, 773–783.
127 H. T. Guo, B. W. Wang, P. Z. Qiu, R. X. Gao, M. M. Sun and L. G. Chen, *ACS Sustainable Chem. Eng.*, 2019, **7**, 8876–8884.
128 J. L. Liu, D. D. Zhu, C. X. Guo, A. Vasileff and S. Z. Qiao, *Adv. Energy Mater.*, 2017, **7**, 1700518.
129 D. M. Zhang, F. Y. Ye, T. Xue, Y. J. Guan and Y. M. Wang, *Catal. Today*, 2014, **234**, 133–138.
130 B. Hu, X. Y. Li, W. Busser, S. Schmidt, W. Xia, G. C. Li, X. B. Li and B. X. Peng, *Chem. – Eur. J.*, 2021, **27**, 10948–10956.
131 L. K. Zhang, X. T. Liu, X. Zhou, S. T. Gao, N. Z. Shang, C. Feng and C. Wang, *ACS Omega*, 2018, **3**, 10843–10850.
132 X. L. Xu, J. J. Luo, L. P. Li, D. Zhang, Y. Wang and G. S. Li, *Green Chem.*, 2018, **20**, 2038–2046.
133 S. S. Cheng, X. F. Meng, N. Z. Shang, S. T. Gao, C. Feng, C. Wang and Z. Wang, *New J. Chem.*, 2018, **42**, 1771–1778.
134 J. Li, S. S. Cheng, T. X. Du, N. Z. Shang, S. T. Gao, C. Feng, C. Wang and Z. Wang, *New J. Chem.*, 2018, **42**, 9324–9331.
135 J. R. Yang, X. H. Qi, F. Shen, M. Qiu and R. L. Smith, *Sci. Total Environ.*, 2020, **719**, 137534.
136 Y. J. Chou, H. C. Ku, C. C. Chien, C. C. Hu and W. Y. Yu, *Catal. Sci. Technol.*, 2020, **10**, 7883–7893.
137 Y. Zhang, L. Chen, Y. Gui and L. Liu, *Appl. Surf. Sci.*, 2022, **592**, 153334.
138 C. K. P. Neeli, P. Puthiaraj, Y. R. Lee, Y. M. Chung, S. H. Baeck and W. S. Ahn, *Catal. Today*, 2018, **303**, 227–234.
139 Z. Liu, W. H. Dong, S. S. Cheng, S. Guo, N. Z. Shang, S. T. Gao, C. Feng, C. Wang and Z. Wang, *Catal. Commun.*, 2017, **95**, 50–53.
140 Y. You, H. Huang, K. K. Mao, S. Xia, D. Wu, C. Y. Hu, C. Gao, P. Y. M. Liu, R. Long, X. J. Wu and Y. J. Xiong, *Sci. China Mater.*, 2019, **62**, 1297–1305.
141 S. S. Li, L. Tao, F. Z. R. Wang, Y. M. Liu and Y. Cao, *Adv. Synth. Catal.*, 2016, **358**, 1410–1416.
142 J. Zhang, Z. J. Wang, M. G. Chen, Y. F. Zhu, Y. M. Liu, H. Y. He, Y. Cao and X. H. Bao, *Chin. J. Catal.*, 2022, **43**, 2212–2222.
143 C. K. P. Neeli, Y. M. Chung and W. S. Ahn, *ChemCatChem*, 2017, **9**, 4570–4579.
144 C. Q. Zhou, Y. Xiao, S. G. Xu, J. M. Li and C. W. Hu, *Ind. Eng. Chem. Res.*, 2020, **59**, 17228–17238.
145 J. Deng, D. H. Deng and X. H. Bao, *Adv. Mater.*, 2017, **29**, 1606967.
146 Z. Y. Yu, Y. Duan, X. Y. Feng, X. X. Yu, M. R. Gao and S. H. Yu, *Adv. Mater.*, 2021, **33**, 2007100.
147 Y. Wang, J. Hao, Y. Liu, M. Liu, K. Sheng, Y. Wang, J. Yang, J. Li and W. Li, *J. Energy Chem.*, 2023, **76**, 601–616.
148 D. T. Tran, D. C. Nguyen, H. T. Le, T. Kshetri, V. H. Hoa, T. L. L. Doan, N. H. Kim and J. H. Lee, *Prog. Mater. Sci.*, 2021, **115**, 100711.
149 S. H. Zhou, F. L. Dai, C. Dang, M. Wang, D. T. Liu, F. C. Lu and H. S. Qi, *Green Chem.*, 2019, **21**, 4732–4747.
150 L. Jiang, P. Zhou, Z. H. Zhang, S. W. Jin and Q. Chi, *Ind. Eng. Chem. Res.*, 2017, **56**, 12556–12565.
151 D. Xu, H. Zhao, Z. P. Dong and J. T. Ma, *ChemCatChem*, 2019, **11**, 5475–5486.
152 Q. Zhu, X. Sun, H. Zhao, D. Xu and Z. P. Dong, *Ind. Eng. Chem. Res.*, 2020, **59**, 5615–5623.

153 H. T. Guo, R. X. Gao, M. M. Sun, H. Guo, B. W. Wang and L. G. Chen, *ChemSusChem*, 2019, **12**, 487–494.
154 M. X. Duan, Q. Y. Cheng, M. M. Wang and Y. J. Wang, *RSC Adv.*, 2021, **11**, 10996–11003.
155 J. W. Zhao, M. R. Liu, G. L. Fan, L. Yang and F. Li, *Ind. Eng. Chem. Res.*, 2021, **60**, 5826–5837.
156 P. Yang, Q. Xia, X. Liu and Y. Wang, *Fuel*, 2017, **187**, 159–166.
157 L. Xu, R. F. Nie, X. J. Chen, Y. C. Li, Y. X. Jiang and X. Y. Lu, *Catal. Sci. Technol.*, 2021, **11**, 1451–1457.
158 L. Xu, X. L. Lyu, Y. X. Jiang, X. W. Wei, R. F. Nie and X. Y. Lu, *Green Chem.*, 2022, **24**, 4935–4940.
159 L. Y. Huang, H. Zhang, Y. J. Cheng, Q. D. Sun, T. Gan, Q. He, X. H. He and H. B. Ji, *Chin. Chem. Lett.*, 2022, **33**, 2569–2572.
160 Z. Gong, Y. Lei, P. Zhou and Z. H. Zhang, *New J. Chem.*, 2017, **41**, 10613–10618.
161 F. W. Zhang, J. J. Li, P. Z. Liu, H. Li, S. Chen, Z. H. Li, W. Y. Zan, J. J. Guo and X. M. Zhang, *J. Catal.*, 2021, **400**, 40–49.
162 H. N. Li, C. Y. Cao, J. Liu, Y. Shi, R. Si, L. Gu and W. G. Song, *Sci. China Mater.*, 2019, **62**, 1306–1314.
163 C. Liu, B. F. Liang, F. L. Jing and S. Z. Luo, *Int. J. Energy Res.*, 2022, **46**, 23682–23697.
164 T. Wang, W. Suo, M. M. Qu, F. Li, S. J. Sun, W. Xue and Y. J. Wang, *J. Chem. Technol. Biotechnol.*, 2022, **97**, 3172–3182.
165 S. Lomate, A. Sultana and T. Fujitani, *Catal. Sci. Technol.*, 2017, **7**, 3073–3083.
166 Y. Sun, C. X. Xiong, Q. C. Liu, J. R. Zhang, X. Tang, X. H. Zeng, S. J. Liu and L. Lin, *Ind. Eng. Chem. Res.*, 2019, **58**, 5414–5422.
167 T. Wang, J. Du, Y. Sun, X. Tang, Z. J. Wei, X. H. Zeng, S. J. Liu and L. Lin, *Chin. Chem. Lett.*, 2021, **32**, 1186–1190.
168 T. Su and C. Cai, *ACS Appl. Mater. Interfaces*, 2022, **14**, 55568–55576.
169 J. Li, C. Li, S. Feng, Z. Zhao, H. Zhu and Y. Ding, *ChemCatChem*, 2020, **12**, 1546–1550.
170 S. Karmakar, S. Barman, F. A. Rahimi, D. Rambabu, S. Nath and T. K. Maji, *Nat. Commun.*, 2023, **14**, 4508.
171 X. D. Li, L. Li, G. B. Chen, X. Y. Chu, X. H. Liu, C. Naisa, D. Pohl, M. Löffler and X. L. Feng, *Nat. Commun.*, 2023, **14**, 4034.
172 M. Zhou, Z. Q. Wang, A. H. Mei, Z. F. Yang, W. Chen, S. Y. Ou, S. Y. Wang, K. Q. Chen, P. Reiss, K. Qi, J. Y. Ma and Y. L. Liu, *Nat. Commun.*, 2023, **14**, 2473.
173 J. Zhou, J. Li, L. Kan, L. Zhang, Q. Huang, Y. Yan, Y. F. Chen, J. Liu, S. L. Li and Y. Q. Lan, *Nat. Commun.*, 2022, **13**, 4681.
174 H. Li, C. K. Cheng, Z. J. Yang and J. J. Wei, *Nat. Commun.*, 2022, **13**, 6466.
175 Y. N. Zhang, C. S. Pan, G. M. Bian, J. Xu, Y. M. Dong, Y. Zhang, Y. Lou, W. X. Liu and Y. F. Zhu, *Nat. Energy*, 2023, **8**, 361–371.
176 X. Q. Yan, M. Y. Xia, H. X. Liu, B. Zhang, C. R. Chang, L. Z. Wang and G. D. Yang, *Nat. Commun.*, 2023, **14**, 1741.
177 T. J. Yan, L. Wang, Y. Liang, M. Makaremi, T. E. Wood, Y. Dai, B. B. Huang, A. A. Jelle, Y. Dong and G. A. Ozin, *Nat. Commun.*, 2019, **10**, 2521.
178 S. Singh, R. Verma, N. Kaul, J. Sa, A. Punjal, S. Prabhu and V. Polshettiwar, *Nat. Commun.*, 2023, **14**, 2551.
179 L. Wang, M. Ghoussoub, H. Wang, Y. Shao, W. Sun, A. A. Tountas, T. E. Wood, H. Li, J. Y. Y. Loh, Y. Dong, M. Xia, Y. Li, S. Wang, J. Jia, C. Qiu, C. Qian, N. P. Kherani, L. He, X. Zhang and G. A. Ozin, *Joule*, 2018, **2**, 1369–1381.
180 W. Qiao, X. Fan, W. F. Liu, F. N. Khan, D. S. Zhang, F. Y. Han, B. H. Yue, Y. J. Li, N. Dimitratos, S. Albonetti, X. D. Wen, Y. Yang, F. Besenbacher, Y. W. Li, H. Niemantsverdriet, H. P. Lin and R. Su, *J. Am. Chem. Soc.*, 2023, **145**, 5353–5362.
181 X. W. Lu, C. M. Guo, M. Y. Zhang, L. P. Leng, J. H. Horton, W. Wu and Z. J. Li, *Nano Res.*, 2021, **14**, 4347–4355.
182 K. Tsutsumi, F. Uchikawa, K. Saka and K. Tabata, *ACS Catal.*, 2016, **6**, 4394–4398.
183 S. H. Dong, Z. Liu, R. H. Liu, L. M. Chen, J. Z. Chen and Y. S. Xu, *ACS Appl. Nano Mater.*, 2018, **1**, 4247–4257.
184 A. K. Kar, A. Behera and R. Srivastava, *ACS Appl. Nano Mater.*, 2022, **5**, 464–475.
185 S. Zhang, Y. X. Liu, M. K. Zhang, Y. Y. Ma, J. Hu and Y. Q. Qu, *Nat. Commun.*, 2022, **13**, 5527.
186 V. Goyal, J. Gahtori, A. Narani, P. Gupta, A. Bordoloi and K. Natte, *J. Org. Chem.*, 2019, **84**, 15389–15398.
187 H.-S. Lee, J. Lee, H. Seo, H. Kang, D. H. Kim and Y.-W. Lee, *Fuel Process. Technol.*, 2021, **218**, 106870.
188 L. Zhu, S. Ye, J. Wang, J. Zhu, G. He and X. Liu, *ChemCatChem*, 2022, **14**, e202101794.
189 V. L. Yfanti and A. A. Lemonidou, *Catal. Today*, 2020, **355**, 727–736.
190 X. Tang, Z. Li, X. Zeng, Y. Jiang, S. Liu, T. Lei, Y. Sun and L. Lin, *ChemSusChem*, 2015, **8**, 1601–1607.
191 Z. Zhang, C. Wang, X. Gou, H. Chen, K. Chen, X. Lu, P. Ouyang and J. Fu, *Appl. Catal., A*, 2019, **570**, 245–250.
192 I. Z. Awan, G. Beltrami, D. Bonincontro, O. Gimello, T. Cacciaguerra, N. Tanchoux, A. Martucci, S. Albonetti, F. Cavani and F. Di Renzo, *Appl. Catal., A*, 2021, **609**, 117929.
193 J. Zhang and J. Chen, *ACS Sustainable Chem. Eng.*, 2017, **5**, 5982–5993.
194 J. Zhang, C. Li, S. Hu, J. Gu, H. Yuan and Y. Chen, *Renewable Energy*, 2022, **200**, 88–97.
195 G. Li, W. Jiao, Z. Sun, Y. Zhao, Z. Shi, Y. Yan, L. Feng, Y. Zhang and Y. Tang, *ACS Sustainable Chem. Eng.*, 2018, **6**, 4316–4320.
196 S. Yao, T. Zhang, X. Tang, D. Li, W. Zhang, D. Lin, R. Li, H. Yan, Y. Liu, X. Feng, X. Chen, X. Zhou and C. Yang, *Energy Fuels*, 2021, **35**, 9970–9982.
197 L. Grazia, D. Bonincontro, A. Lolli, T. Tabanelli, C. Lucarelli, S. Albonetti and F. Cavani, *Green Chem.*, 2017, **19**, 4412–4422.
198 H. Zhang, X. Tong, Y. Gao, H. Chen, P. Guo and S. Xue, *J. Ind. Eng. Chem.*, 2019, **70**, 152–159.

199 L. Luo, X. Han and Q. Zeng, *Catalysts*, 2020, **10**, 1096.
200 X. Wu, J. Li, S. Xie, P. Duan, H. Zhang, J. Feng, Q. Zhang, J. Cheng and Y. Wang, *Chem*, 2020, **6**, 3038–3053.
201 Y. B. Zhao, F. Pan, H. Li, G. Q. Xu and W. Chen, *ChemCatChem*, 2014, **6**, 454–458.
202 Y. M. Jian, Y. Meng, J. Li, H. G. Wu, S. Saravanamurugan and H. Li, *J. Environ. Chem. Eng.*, 2022, **10**, 108837.